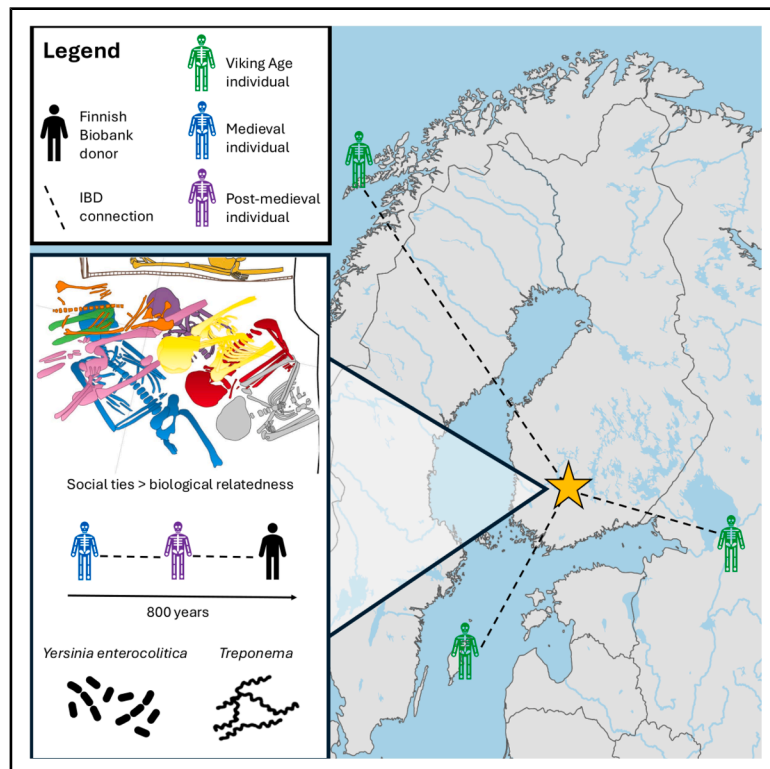


Archaeogenetics reveals fine-scale genetic continuity and patterns of kinship and health in medieval Finland

Graphical abstract



Authors

Ulla Nordfors, Sanni Peltola, Ronan James O'Sullivan, ..., Johannes Krause, Elina Salmela, Päivi Onkamo

Correspondence

ulla.nordfors@utu.fi (U.N.),
sanni.peltola@helsinki.fi (S.P.)

In brief

Classification Description: Human genetics; Biological sciences; Paleobiology; Anthropology

Highlights

- Genome-wide ancient DNA data from medieval and post-medieval Finland
- Identity-by-descent (IBD) reveals population continuity for at least 800 years
- Patterns of relatedness suggest the importance of social ties in burial practices
- Potential cases of *Yersinia enterocolitica* and *Treponema*



Article

Archaeogenetics reveals fine-scale genetic continuity and patterns of kinship and health in medieval Finland

Ulla Nordfors,^{1,2,3,7,8,*} Sanni Peltola,^{1,3,4,5,7,*} Ronan James O'Sullivan,^{1,5} Aida Andrades Valtueña,⁵ Theseas C. Lamnidis,⁵ Kerttu Majander,⁶ Luca Traverso,⁵ Johannes Krause,⁵ Elina Salmela,^{1,2,5} and Päivi Onkamo¹

¹University of Turku, Department of Biology, Turku, Finland

²University of Turku, Department of Archaeology, Turku, Finland

³Museum Centre Vapriikki, Tampere, Finland

⁴Faculty of Biological and Environmental Sciences, University of Helsinki, Helsinki, Finland

⁵Department of Archaeogenetics, Max Planck Institute for Evolutionary Anthropology, Leipzig, Germany

⁶Department of Environmental Sciences, University of Basel, Basel, Switzerland

⁷These authors contributed equally

⁸Lead contact

*Correspondence: ulla.nordfors@utu.fi (U.N.), sanni.peltola@helsinki.fi (S.P.)

<https://doi.org/10.1016/j.isci.2025.113086>

SUMMARY

We investigated ancestry, kinship, and health in individuals from three cemeteries in Finland: Tampere Vilusenharju and Pälkäne Ristiänmäki (11th–12th centuries) and Rauniokirkko (13th–19th century). The oldest burials provide insights into Finland's medieval population, otherwise poorly known due to poor bone preservation. Using ancient genomic data, contemporary Finnish Biobank data, and identity-by-descent (IBD) analyses, we identified strong regional continuity between the medieval and modern Finnish populations and evidence for mobility within Finland and between Finland and Scandinavia. Kinship analysis identified a sibling relationship between individuals buried 30 km apart and indicated a shared genetic background for individuals from the three cemeteries. However, individuals buried in physical proximity at Rauniokirkko were not closely related, suggesting that social ties, not family relations, shaped burial practices. The pattern may reflect emerging Christian mortuary norms and community-based burial organization. Pathogen screening revealed potential *Yersinia* and *Treponema* infections, shedding light on disease burden in medieval Finland.

INTRODUCTION

The Medieval period in Finland spans from ca. 1150 to 1527 CE.¹ One of the most defining features of the period was the Christianization of Finland. This religious transformation was part of broader religious developments across Scandinavia and the Baltic region, and it led to new burial practices as cremation was abandoned in favor of inhumation. New governance structures and legal frameworks also laid the groundwork for Finland's integration into the broader Scandinavian and Roman Catholic world.

At the beginning of the medieval period, Finland's estimated population size was 20,000–40,000 people.² This population was concentrated in permanent agricultural settlements primarily along the southern and western coastlines and at inland sites in Satakunta, Häme (also called Tavastia) and Southern Savo (also called Savonia), where the climate and soil conditions favored arable cultivation.³ The northern inland areas featured non-permanent settlements that were used for seasonal hunting and fishing, and mobile Sámi groups were likely present further south than the Sámi are today.^{4,5} As the population grew to around 300,000 by the late 16th century, the increased land demand spurred migrations, especially from Southern Savo to

more northern regions, with slash-and-burn agriculture facilitating this expansion.

The Finnish population has been extensively studied with respect to medical and population genetics due to its relatively small population size and relative isolation and comprehensive national population registers.^{6–8} This interest has yielded a growing resource of genetic data from present-day Finland (e.g., Ref.⁹, finngen.fi), but ancient-DNA studies from the region are scarce due to the country's historically low population size^{10,11} and the acidic soil leading to poor bone preservation.¹ Consequently, research material from Finnish medieval sites is typically limited compared to other European sites.

In this study, we examined 25 individuals from three medieval burial sites in Finland: Tampere Vilusenharju, Pälkäne Ristiänmäki, and Pälkäne Rauniokirkko (St. Michael's Church; Figure 1). The sites are located in the historical border region of Upper Satakunta and Häme, which are among the areas with longest continuous settlement in Finland.³ The region is today part of Pirkanmaa province, which is why we use this name for the area in this article. We leveraged the extensive modern Finnish biobank data to examine the genetic history of medieval Pirkanmaa at a fine scale. We found local genetic



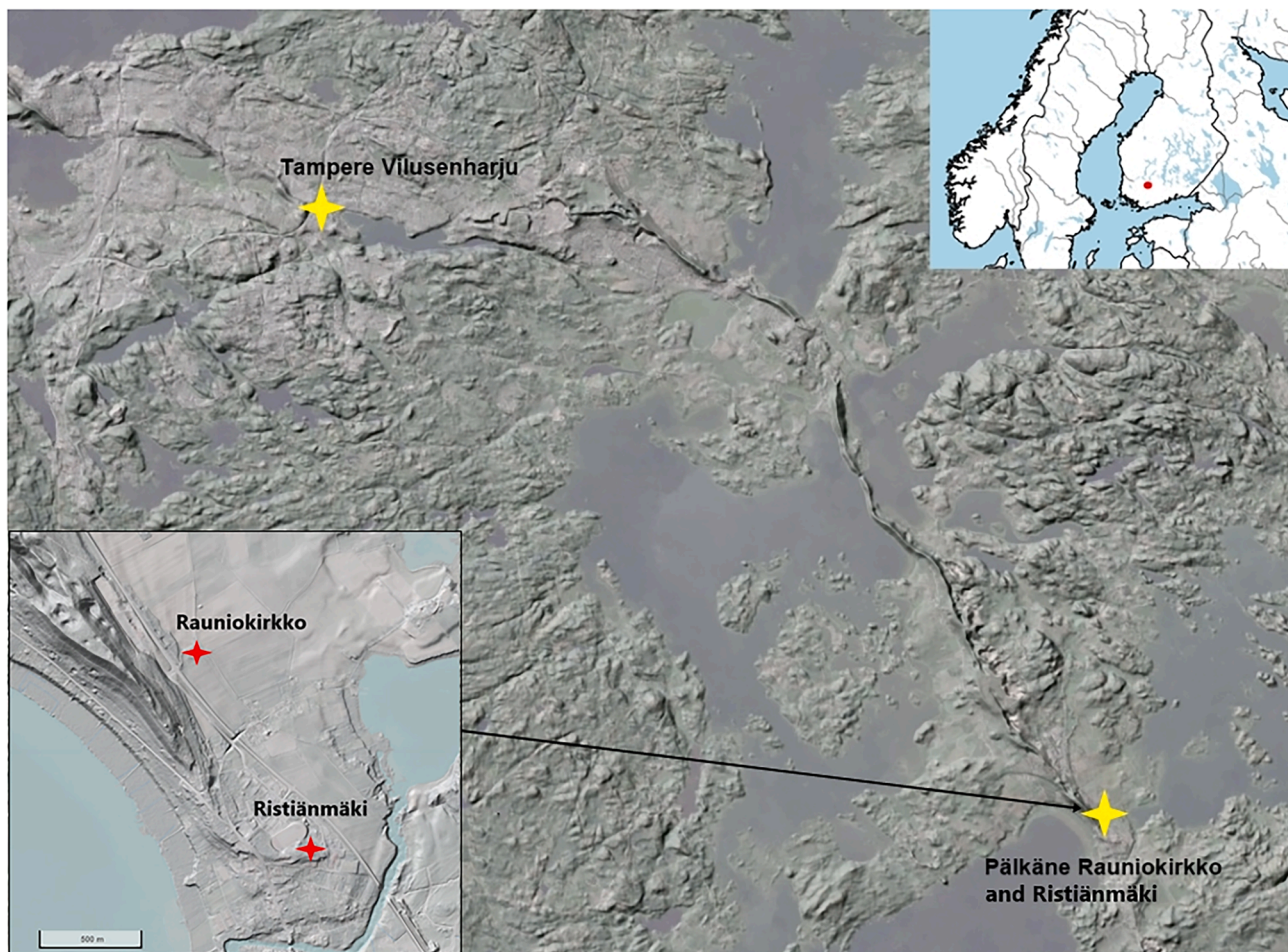


Figure 1. The location of Tampere Vilusenharju, Pälkäne Rauniokirkko, and Ristiänmäki and the surrounding topography with the clearly distinguishable esker between the sites

The eskers at and around Vilusenharju were removed in sand extraction in the 1960s and 1970s, and the area is now an urban area within the city of Tampere. The cemeteries of Rauniokirkko and Ristiänmäki are located approximately 1 km apart. Ristiänmäki was used between the 11th and 13th centuries and Rauniokirkko from the 13th century to the 1840s. The exact chronology between the sites is unknown—it is still undetermined whether burial at Ristiänmäki stopped when it began at Rauniokirkko or whether the sites were used simultaneously in the 13th century.

continuity from the Middle Ages to present day and also demonstrated the power of large reference panels and identity-by-descent (IBD) analyses in detecting individual mobility. We estimated population size, inferred kinship patterns, and explored connections between medieval Finland and Scandinavia. Finally, we discovered potential cases of infectious disease, which illustrated the life and health of these medieval agricultural communities. We also identified known variants affecting phenotypic traits and genetic predispositions of the individuals. This information can be utilized in a museum exhibition as an additional tool to portray past people as distinct individuals.

RESULTS AND DISCUSSION

Insights into the ancestry of medieval and post-medieval Pirkanmaa

We screened ancient DNA preservation of 25 individuals from medieval and post-medieval Pirkanmaa. Samples with at least

0.1% endogenous DNA were enriched for 1.2 million genome-wide markers. Out of the 25 samples, 20 had sufficient DNA preservation to yield genome-wide pseudohaploid data, ranging from 17,659 to 79,0569 markers overlapping the 1.2 million genome-wide markers in the enrichment panel (Table S1). Out of those 20, 14 had sufficient post-imputation quality (see Materials and Methods) and could be used in IBD analyses. We consider the level of DNA preservation in our samples better than expected in the context of Finland. This was likely influenced by the fact that the samples were taken directly from the excavation, rather than having been stored in a museum environment (cf. Ref.¹²; see also Figure S1).

We used pseudohaploid data for exploratory analyses and F statistics. In the West Eurasian PCA space, most ancient Pirkanmaa individuals clustered among or close to present-day Finns (Figure S2; Table S2). ADMIXTURE¹³ analysis showed similar ancestry composition between ancient individuals and present-day Finns (Figure S3). In outgroup F₃ statistics, the ancient group

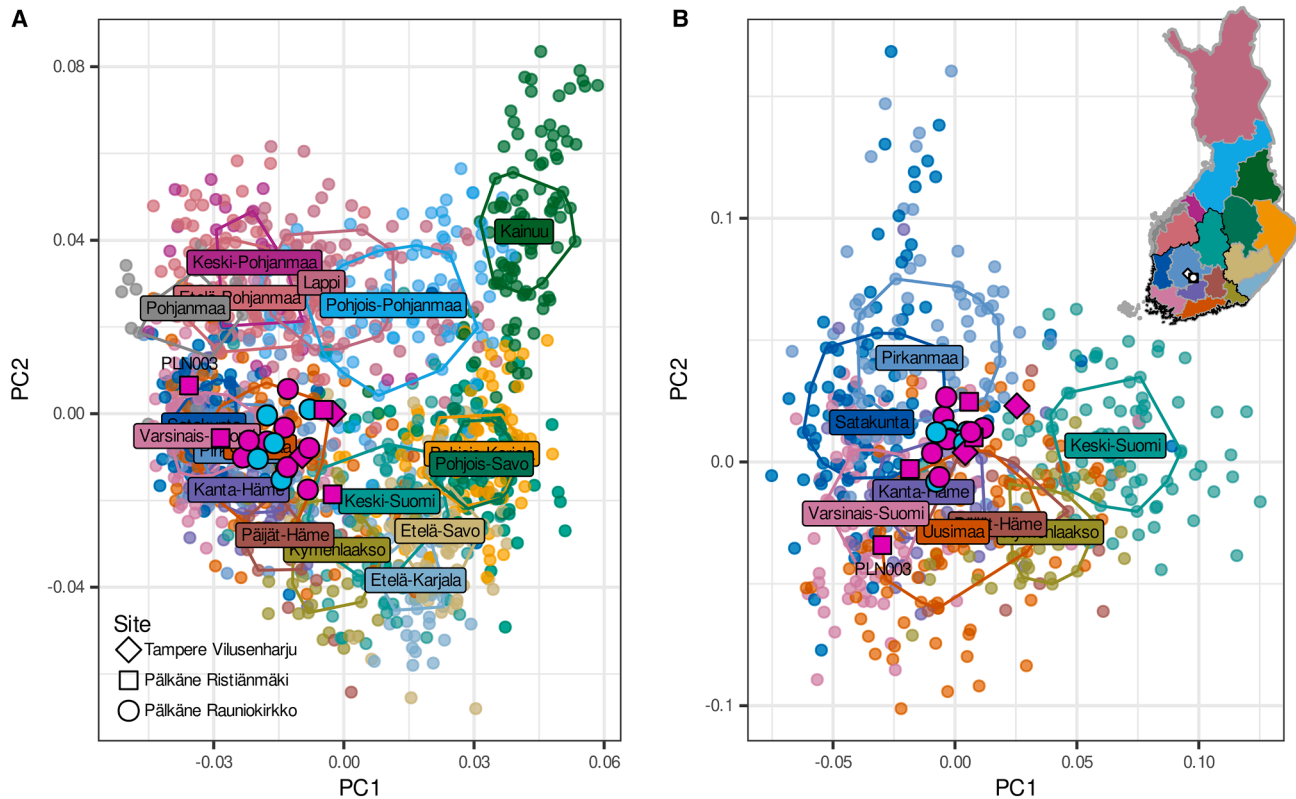


Figure 2. Principal-component analysis (PCA) of modern and ancient individuals from Finland

PCA represents genetic variation in present-day Finns A., throughout the country ($n = 1487$), and B., from southwestern provinces ($n = 588$). Points denote present-day individuals grouped by their parental birth province. Labels show median PCA coordinates and convex hulls enclose the 50% of points closest to the geometric mean per group. Medieval (magenta) and post-medieval (cyan) genomes from Pälkäne and Vilusenharju are projected on top of the present-day variation.

shared most genetic drift with present-day Karelians, Veps, and Finns (Table S3). On a PCA that captures the present-day variation within Finland, the ancient individuals fall among present-day southwestern Finns (Figure 2A; Table S4). In the context of southwestern Finland, the majority of the individuals clustered tightly in the plot area between the present-day Pirkanmaa, Häme, and Satakunta regions, parallel to their discovery location. This suggests genetic continuity on the regional scale (Figure 2B).

One individual, PLN003, was consistently shifted away from the main group in all PCAs (Figures 2 and S2). On the West Eurasian PCA, PLN003 falls close to the East European populations and shares more alleles with Czech and Estonians than with Finns in outgroup F_3 tests, possibly indicating gene flow from a group outside Finland (Figure S2; Table S3). However, a contMix¹⁴ analysis estimated that the sample has 6.5% mitochondrial contamination (Table S1), and although mitochondrial contamination estimate from Renaud et al.¹⁵ was not alarming, we cannot rule out the possibility of contamination affecting the individual's ancestry estimates.

Population continuity between medieval and post-medieval Pirkanmaa

To investigate potential shifts in ancestry over time, we divided the samples into two temporal clusters: medieval and post-

medieval. Individuals dating to the 12th–15th centuries were labeled medieval, whereas the rest, dating from the 16th–19th century, were labeled post-medieval (see Table S1). First, we calculated outgroup F_3 statistics for pairs of individuals within each group (Table S5) but found no significant difference between the within-group mean F_3 estimates (permutation test with 1,000,000 replicates, $p = 0.18$), indicating similar levels of genetic diversity within both the medieval and post-medieval group.

We then examined differential allele sharing of the two groups with present-day Finns. For this, we calculated two sets of F_4 statistics in the form of $f_4(\text{Mbuti.DG}, \text{Test}; \text{Temporal_group}, \text{Finnish.DG})$, where *Test* represents 162 present-day non-African populations and *Temporal_group* represents either the medieval or the post-medieval Pirkanmaa group. We found that both groups showed slightly more affinity to present-day East Asian groups than present-day Finns do (Figure S4; Table S6). However, we have no information on the geographic origin of the genomes representing present-day Finns in these calculations, and it is thus possible that we recover a spatial difference rather than a temporal one.

To explore the temporal patterns in allele sharing at a local scale, we calculated outgroup F_3 statistics between each of the two temporal groups and present-day Finns from 12 subregions (Table S7). Both groups shared most alleles with

present-day Central Finland instead of present-day Pirkanmaa, which ranked fourth (Table S8). Finally, we compared the temporal groups directly by computing F_4 statistics in the form of $f_4(\text{Mbuti.DG, Test; Pirkanmaa_medieval, Pirkanmaa_post_medieval})$, where *Test* represents the 12 Finnish subregions. We found no statistically significant difference between the two temporal groups relative to 12 Finnish subregions (Table S8).

We examined population continuity from the medieval and historical periods to the present day. To test for symmetrical relatedness of ancient Pirkanmaa to present-day inhabitants of the nearby regions, we calculated F_4 statistics in the form of $f_4(\text{Mbuti.DG, Test; Temporal_group, Regional_group})$, where *Regional_Group* was substituted with a geographically proximal present-day group (Pirkanmaa, Häme, or Central Finland) and *Test* with the remaining Finnish regional groups (Table S7). None of the calculated F_4 estimates were significantly negative, suggesting lack of substantial gene flow from other regions to Pirkanmaa between the medieval-historical era and present day (Table S8).

Connections to present-day Finland

To examine population continuity at a fine scale, we studied IBD sharing between the archaeological individuals and present-day Finns (Table S4; Materials and Methods). For these analyses, imputed data from 14 ancient Pirkanmaa individuals were used (Table S1). Due to their temporal distance, individual IBD connections between the archaeological and modern individuals should not be interpreted as relatedness in a common sense. Rather, the geographical distribution of these connections can be used as evidence for population-level common ancestry. We used municipality-level mean sums of IBD segment length as a statistic to represent genetic connectivity between ancient Pirkanmaa and present-day Finns, and these statistics were then used to estimate IBD connectivity across Finland using kriging interpolation or inverse distance weighting (see Materials and Methods). Our results reveal a very localized pattern of IBD connectivity that peaks in present-day Pälkäne, where nearly all samples included in the IBD analysis were excavated (Figure S5). This demonstrates a strong persistence of lineages in the same region for at least 800 years. We did not detect major shifts in connectivity between the medieval and post-medieval groups, which is consistent with our previous F -statistics that suggested continuity between the two temporal groups.

We noted that some segments shared by the archaeological and the present-day individuals had identical boundaries, i.e., the segment shared with an ancient individual was also shared by two or more present-day individuals. Approximately 5% of the segments appeared in the present-day population dozens of times. We assume that these “common” segments likely represent deeper shared ancestry in Finland, whereas rare segments may represent more recent lineages. Thus, rare segments could reveal patterns parallel to rare allelic variants, which are more geographically stratified and thus more powerful than common variation for studies of fine-scale population structure.¹⁶ To study this further, we repeated the above analyses for the “common” and “rare” segment categories separately (see Material and Methods for details) and found that the two segment categories had distinctive spatial distributions: common segments

showed a more wide-spread pattern (Figure 3A), roughly parallel to the pattern of allele sharing from outgroup F_3 statistics (Table S8). Rare segments, on the other hand, were strikingly focused at Pälkäne (Figure 3B). These patterns are consistent with the assumption that the rare segments capture local, and potentially more recent, lineages.

To identify potential outliers and individual mobility, we analyzed the spatial pattern of “rare,” “common,” and overall IBD connectivity separately for each individual. The majority of individuals had highest rare-IBD connectivity in Pirkanmaa, Häme, or more broadly in south-western Finland (Figure S6). However, one individual, JK2285, had only minor connectivity to Southwestern Finland and highest connectivity to Central Ostrobothnia. Another individual, PKN006, had high connectivity to Southern Savo in addition to connections to Southwestern Finland. Two individuals, TMP003 and PLK003, further showed connectivity to Southeastern Finland in their common IBD connectivity, despite having highest rare-IBD sharing in Pirkanmaa. However, inferring timing and directionality of movement from these patterns is not straightforward, since the spatial distribution of IBD sharing could be affected by the mobility of the descendant population. Understanding the origin and trajectories of individual segments under different demographic scenarios would require simulations and in-depth analysis of coalescent times, which were outside the scope of this study. Nevertheless, using unique segments as a proxy, we can already grasp patterns of fine-scale population structure.

Social practices and population size

Kinship analysis of individuals buried at Pälkäne Rauniokirkko provides insights into funerary practices and familial connections in medieval Finland. We used pseudohaploid data and READv2¹⁷ to analyze close genetic relatedness within the set of samples. Among the individuals sampled from Rauniokirkko, four were children (PLN001, PKN010, PKN013, and PKN014), whereas the rest ($n = 17$) were adults (Table S1). Interestingly, six of the medieval adults (PKN002, PKN003, PKN005, PKN006, PKN008, and PKN009) were buried in a small, confined area, overlapping each other in four distinct layers.¹⁸ According to radiocarbon dating, all of these burials were made in the 13th century, suggesting that despite the availability of space, the people deliberately chose to bury these adults in tightly packed layers. The interments were separated by years or even decades, except the grave of two individuals (PKN005 and PKN006), who were buried simultaneously in a double grave at the end of the century.

The arrangement of the 13th-century burials in a confined area and in overlapping layers was initially interpreted as a potential family grave. However, genetic analysis did not reveal close biological relationships among the individuals (Table S9). One double grave contained individuals PKN005 (XX) and PKN006 (XY), with a notably intimate positioning: PKN006 lay on his left side facing PKN005, with one hand under her shoulder and the other across her elbow. Such bodily contact has often been interpreted as indicative of a close interpersonal relationship,^{19,20} possibly suggestive of a pair bond. Nonetheless, not all significant social relationships are genetically based. In this case, the absence of kinship ties among all the individuals in the cluster

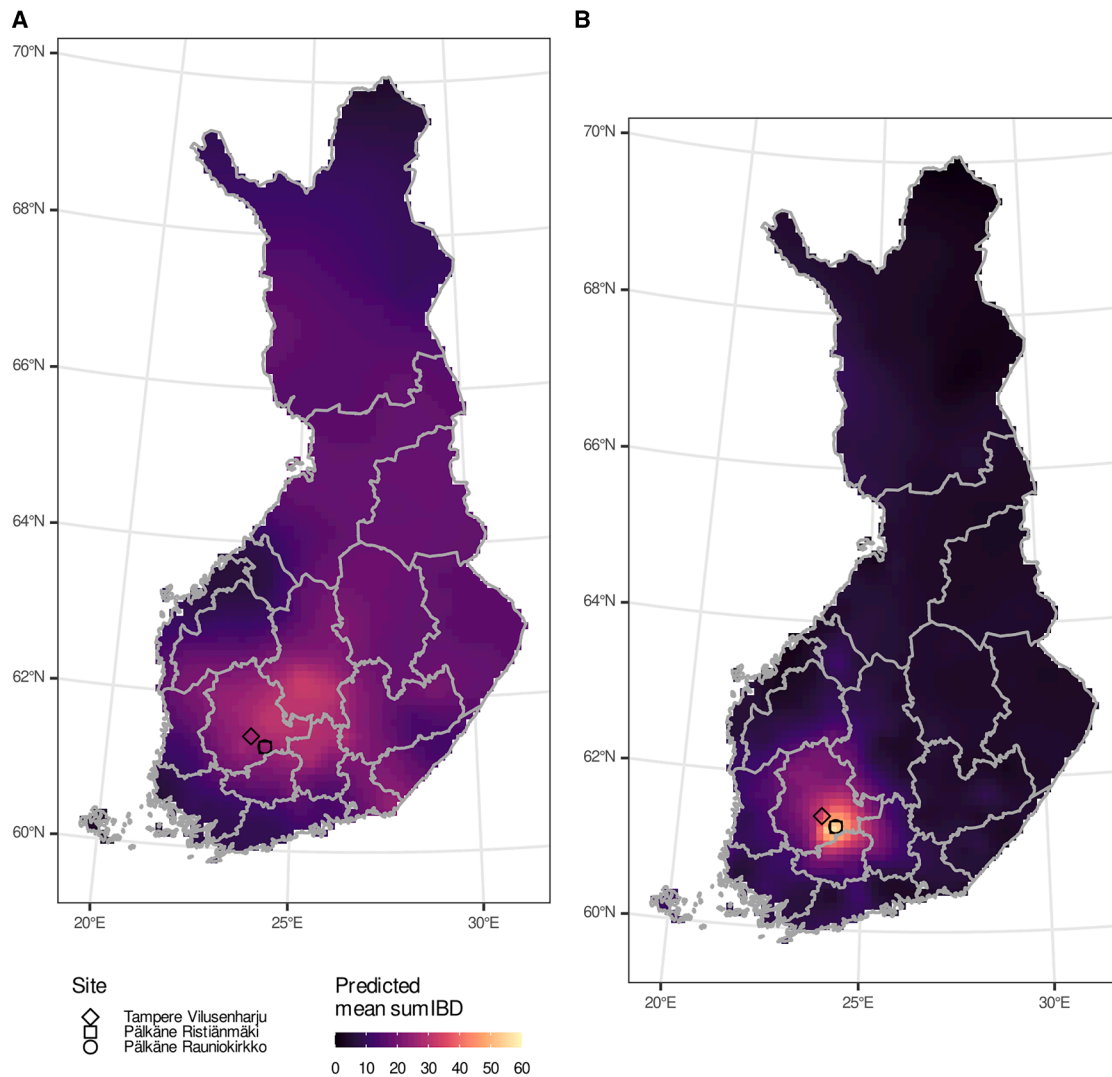


Figure 3. Spatial distribution of IBD connectivity between the ancient Pirkanmaa individuals and present-day Finns

Normalized sums of IBD segment lengths between 14 ancient individuals and the present-day individuals from each municipality are used for spatial kriging. Map shows interpolated values; higher values indicate stronger IBD connectivity between the ancient and present-day people.

(A) “Common” segments with shared chromosomal start or end coordinates.

(B) “Rare” segments with unique chromosomal start and end coordinates.

raises the possibility that some other social principle was behind the burial pattern. One possible interpretation is the shared religious identity of the deceased. By the 13th century, the Christianization of the Häme region was underway, marked by the establishment of the first ecclesiastical parishes and churchyards.^{21,22} Although written documentation is sparse for this period, archaeological evidence suggests that Christian mortuary practices—such as standardized body orientation and burial in consecrated ground without artifacts—were becoming increasingly prevalent.¹ In Christian ideology, the dead were conceptualized as members of a spiritual community that extended beyond familial ties. The grouping of these burials could therefore reflect membership in an emerging Christian congregation, where moral status or ritual inclusion (“good

Christians”) determined the location of the burial.²³ In this light, the Rauniokirkko burials may provide rare material evidence of early Christian community formation in inland Finland.

Significantly, the only first-degree kinship—full siblings—was detected between two individuals from cemeteries 30 km apart: an adult female at Vilusenharju (TMP002) and an adult male at Ristiänmäki (PLN004) (Table S9). They also share a relatively rare mtDNA haplogroup in Finland, Z1a1a, further confirming their relatedness (Table S1). The cultural similarities between the sites indicate interactions and exchanges between the people in the region. The sites are also geographically connected by a long esker that stretches between the sites (Figure 1), and this natural pathway likely encouraged movement between the areas.

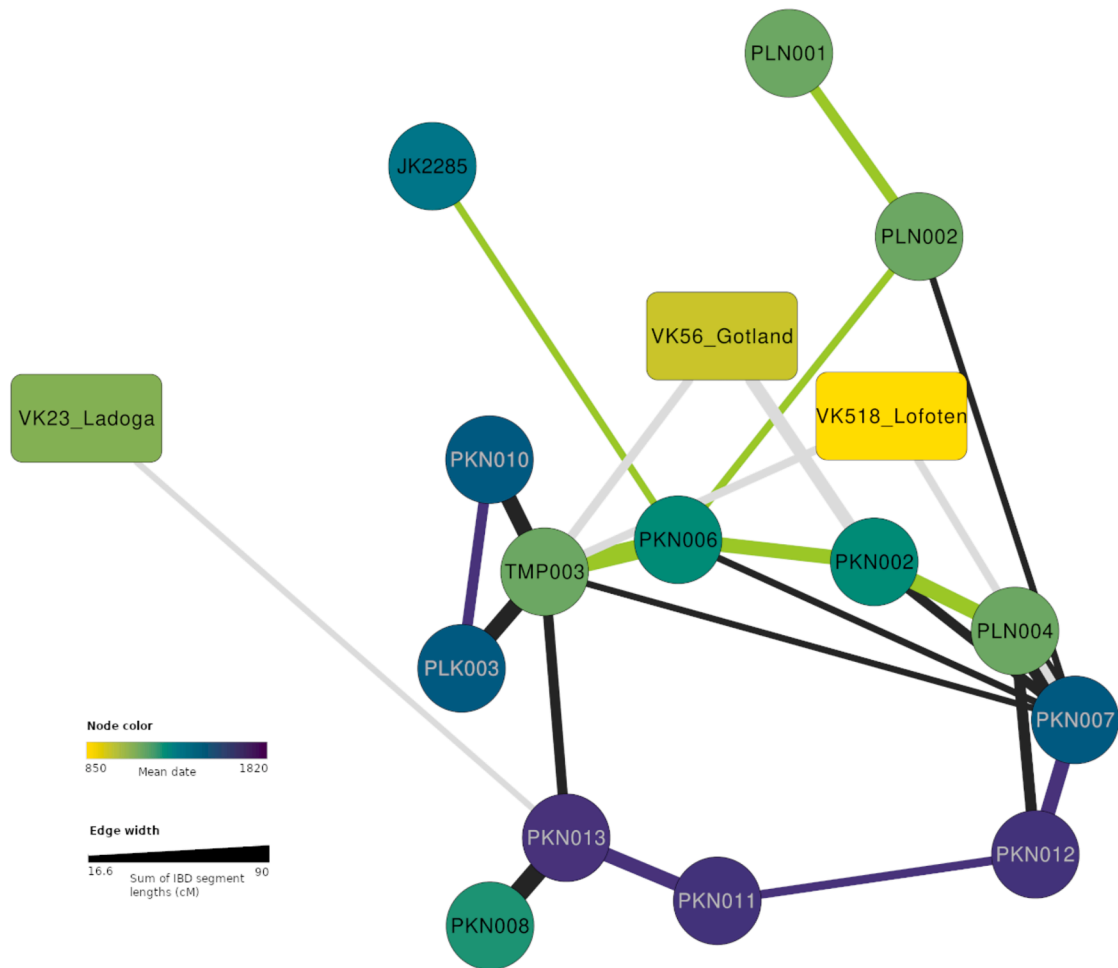


Figure 4. IBD connections discovered between the newly sequenced individuals and published data

Edge thickness indicates the total length of shared IBD segments between a pair (not in scale). Edge color indicates pairs within a temporal group (green: medieval-medieval; blue: post-medieval-post-medieval), black edges are connections between medieval and post-medieval individuals; gray edges indicate connections to individuals buried outside Finland. cM, centimorgan.

To study more distant relatedness within the ancient Pirkanmaa group, we used *ancIBD*²⁴ to call IBD segments between the 14 individuals who had sufficient data for imputation (Table S1). This analysis included imputed genomes of 10 individuals from Pälkäne Rauniokirkko, 3 individuals from Pälkäne Ristiänmäki, and only 1 individual from Tampere Vilusenharju (TMP003). We found that all these individuals shared an IBD connection to at least one other individual in this dataset (Figure 4; Table S10), but none were closely related. The exact degree of relatedness is not possible to determine for such distant relatives, and it could be further affected by background relatedness in the population. Importantly, half of the 20 connections among the 14 individuals were found between medieval and post-medieval individuals. Within-group IBD sharing was similar in both temporal groups.

We modeled the effective population size of ancient Pirkanmaa by analyzing runs of homozygosity (ROH) and using a maximum likelihood framework implemented in *hapROH*.²⁵ For

this analysis, we used pseudohaploid data but included only individuals with >400,000 SNPs. Long ROH indicate parental relatedness (consanguinity) while shorter tracks of ROH are usually a sign of a more distant relatedness, often caused by a relatively small population size. We detected short ROH in nearly all of the 14 analyzed individuals, but none carried large sums of long ROH (>20 cM), which would be indicative of parental relatedness within a few previous generations (Figure S7). The pattern is consistent with more distant background relatedness, typical for small population size.

Effective population size was estimated to be 1,847 (95% confidence interval [CI]: 1,228–2,956) individuals. This estimate is an average over several centuries; the individuals included in the estimation have a mean date at mid-15th century. Previous estimates for effective population sizes of historical Häme (which includes the current provinces of Pirkanmaa, Kanta-Häme, and Päijät-Häme), derived from present-day genetic data,²⁶ suggest that in the mid-15th century the effective population size in this

region was around 12,000. However, this estimate represents the effective population size over a much larger region, while our analysis focused on individuals buried mostly in one municipality. Furthermore, the previous estimate is based on IBD sharing, whereas we use ROH, which may be less accurate for population size estimation. More ancient samples would be needed to model the effective population size and its changes through time with IBD sharing.

We note that, although all individuals are part of the same IBD network and carry varying levels of short ROH, we did not detect individuals who would be a result of recent inbreeding and found only one close genetic kinship (Figures 4 and S7; Tables S9 and S10). This could indicate that the medieval communities had social practices to actively avoid close-kin unions. Such practices have been inferred from population record data from 19th and early 20th century Finland, where first-cousin marriages were significantly less frequent than expected in a randomly mating population.²⁷ Alternatively, the observed patterns of frequent but short ROH and high levels of distant IBD sharing but no close relatives could be explained by recent population growth that took place in the medieval period.

Potential connections to Scandinavia

From an archaeological perspective, Finland had close contacts with Sweden throughout the Iron Age.^{3,28} These ties further intensified in the medieval period through the spread of Christianity and political integration of Finland into the Kingdom of Sweden. Before the 1400s, Swedish settlers moved into coastal regions of Finland, and based on toponyms and personal names, Swedish and German influence, possibly also inhabitants, arrived in the Finnish region throughout the Middle Ages.²⁹

We used Ralph et al.³⁰ to call Y chromosome haplogroups from BAM files for the genetically male individuals in our dataset and found that all of them fall in three major lineages, I1a, N1a, and R1a (Table S1). Six out of ten males carried I1a haplogroups. I1a is the second most common haplogroup in modern Finland, most frequent in the country's southwestern coast. The spatial distribution of I1a is commonly seen as a result of gene flow from Scandinavia, where the frequency of I1a peaks globally.³¹ Somewhat surprisingly, only one individual carried N1a1, the most common haplogroup in modern Finland,³² although another low-coverage individual also likely falls within this lineage (low-resolution haplogroup defined to N1a). The remaining two individuals carried R1a haplogroups, found in approximately 4% of present-day Finnish men.

Compared to our dataset, the frequencies of I1a are substantially lower in the present-day male population of Pirkanmaa and Häme, 28% and 12%, respectively. N1a1 constitutes over 60% of paternal lineages in these regions. The high frequency of haplogroup I1a could be interpreted as Scandinavian influence, but later gene flow from the east, where N1a1 has the highest frequency in Finland, could also explain the apparent changes in frequencies. These two explanations are not mutually exclusive. However, given the strong local continuity in the Pälkäne region, I1a might also have a long history in the area, but putative local pockets of I1a cannot be detected from the province-level averages. Denser sampling of the modern population would be needed to study municipality-level variation in the paternal line-

ages. Moreover, more ancient samples would be needed to make meaningful and statically sound statements about potential temporal shifts in the paternal lineages.

Genome-wide IBD sharing offers yet another piece of evidence of Scandinavian connections. In ancIBD analysis, we found connections between the imputed Pirkanmaa individuals and two published genomes from the Viking-Age Scandinavia³³ (Table S2). Two of the medieval individuals (TMP003 and PKN002) have an IBD connection to a Viking-Age individual from Gotland, and two (TMP003 and PKN007) share IBD segments with an individual from Lofoten in Northern Norway (Figure 4; Tables S2 and S10). Importantly, both mentioned Viking-Age individuals—despite being found in a non-distinctive, regular Viking Age archaeological context—are genetically not typical Scandinavians. The individual from Lofoten carries Sámi-related ancestry, whereas the Gotland individual was described as genetically “Finnish” by the authors. Previous studies have demonstrated that the increased maritime mobility resulted in the higher genetic diversity in Viking Age Scandinavia compared to preceding or succeeding time periods and genetic influx of Central European, Britain-related, and Baltic ancestries.^{33–36} Thus, the observed connections between Viking-Age individuals in Scandinavia and medieval individuals in Finland likely reflect individual mobility from Finland to Scandinavia during the Viking Age. Viking Age mobility also brought Scandinavian ancestry to many regions outside Scandinavia, possibly including Finland, but our IBD analysis was not able to capture such mobility. Properly assessing Scandinavian gene flow to Finland would require ancient DNA from individuals from Finland who predate the Viking Age.

Sámi-related ancestry

IBD connections between medieval Finland and Viking Age Sámi-related individuals reveal potential connections between Finnish and Sámi populations. Present-day Finns, Sámi, and other Uralic-speaking populations in the Baltic area are known to carry significant proportions of Siberian-related ancestry, best represented by present-day Nganasans from the Taymyr Peninsula.^{37–39} Siberian-related ancestry is nearly absent from their non-Uralic neighbors. In Northern Finland, recent intermarriages between the Finns and the Sámi are well known, but interactions between Finnish and Sámi-related groups in southern Finland are elusive. The presence of Sámi-related groups in southern Finland is attested by the Sámi-related ancestry carried by Iron-Age individuals from Leväluhta in Southern Ostrobothnia, as well as toponyms that originate from Sámi languages.

Contribution from Sámi-related groups could explain the subtle eastern affinity of the ancient Pirkanmaa individuals. We tested this by calculating outgroup- F_3 statistics in the form of $f_3(\text{Test}, \text{Individual}; \text{Mbuti.DG})$, where *Test* was either present-day Nganasan, Sámi, or the Viking-Age individual VK518 from Northern Norway, for each ancient and 14 present-day individual from Pirkanmaa-Häme region (Figure S8A; Tables S5 and S10). Visual comparison of the resulting F_3 estimate distributions did not indicate a difference in Sámi-related ancestry in ancient and present-day groups. We assessed the group-level differential affinity to Sámi-related sources directly by calculating F_4 statistics in the form of $f_4(\text{Mbuti.DG}, \text{Sámi-related source};$

ancient group, present-day group) and f_4 (Mbuti.DG, Sámi-related source; Pirkanmaa_medieval, Pirkanmaa_post-medieval). None of the estimates were statistically significant, although we noted that medieval Pirkanmaa showed a consistent trend of having more affinity to all Sámi-related sources than post-medieval and present-day groups did (Figure S8B; Table S11).

Although we did not find a significant temporal difference in the mean affinity of Sámi-related ancestry, individuals who lived closer to the time of admixture could exhibit more variation in their Sámi-related ancestry proportions. To assess this, we calculated F_4 statistics in the form of f_4 (Mbuti, Sámi-related; individual1, individual2), where the two individuals were both either from the modern or ancient group. We found only four pairs that were significantly (Z score >3) more differentially related to any of the Sámi-related groups (Figure S8C; Table S11). Notably, we found two pairs in both ancient and modern groups, indicating that ancient individuals did not have more variation in their Sámi-related ancestry proportions than present-day individuals from the same region. Thus, we conclude that majority of the Sámi- or Siberian-related ancestry in the Pirkanmaa-Häme region stem from admixture events that occurred well before early medieval times.

Pathogen finds illuminate health in a medieval community

We screened all shotgun and captured sequencing data with the metagenomic screening pipeline HOPS⁴⁰ as implemented in *nf-core/eager*⁴¹ for potential human pathogen DNA. This analysis yielded indications of possible infection in five individuals (Tables S12 and S13). Three of these individuals—PKN005 (a young adult female from a 13th-century double grave), PKN010 (a 16th-century child), and JK2287/PLK003 (a 16th-century adult male)—exhibited bacterial sequences assignable to the *Yersinia* genus. This genus includes multiple pathogenic species, most notably *Yersinia pestis*, the etiological agent of plague. To assess the possibility of plague specifically, we performed competitive mapping against several *Yersinia* species and the three virulence-associated plasmids characteristic of *Yersinia pestis*, following the protocol of Andrades Valtueña et al.⁴² (see Materials and Methods; Table S14). All individuals yielded negative competitive *pestis* scores. With the exception of PKN005, none had any sequence reads aligning to the *Y. pestis*-specific plasmids. In PKN005, only a few such sequences were found and not at levels that would indicate infection. Taken together, these results strongly suggest that the individuals were not infected with plague. This interpretation is further supported by historical evidence: there is no confirmed presence of plague in Finland prior to the late 15th century,⁴³ making a 13th-century case (PKN005) highly unlikely.

Instead, the observed sequences are more plausibly attributed to *Yersinia pseudotuberculosis* (PKN005) and *Yersinia enterocolitica* (PKN010, JK2287/PLK003). Both species can cause gastrointestinal and systemic infections in humans, particularly in environments where close contact with livestock or poor sanitation enables zoonotic transmission. These bacteria are commonly associated with pigs and cattle and are typically transmitted through contaminated food, water, or direct contact with animals.^{44,45} In medieval agricultural societies, where hy-

giene practices were limited and people often shared close quarters with domestic animals, the risk of *Yersinia* infections would have been elevated. However, *Y. pseudotuberculosis* and *Y. enterocolitica* are also commonly found in soil,^{44,46} which means that environmental contamination cannot be completely ruled out.

Further evidence of microbial presence was found in two individuals. A 13th-century male (PKN006), interred in a double grave, and a 19th-century child (PKN013) yielded sequences attributed to *Streptococcus* spp. (Table S13). In both cases, DNA was extracted from dental tissue, and the sequences likely derive from oral microbiota. Specifically, PKN006 exhibited *Streptococcus mutans*, a common inhabitant of the oral cavity. This individual also showed potential evidence of *Neisseria meningitidis* (Table S13), a human-specific pathogen capable of causing meningitis and sepsis.⁴⁷ However, up to 10% of the present-day population carry the bacteria in their nasopharynx, most without symptoms. Since the relevant sequences were recovered only from PKN006's dental calculus and not from dentine, they likely represent asymptomatic colonization.

Lastly, individual PKN012, an adult male from a 19th-century burial, exhibited genetic traces consistent with *Treponema pallidum*, the causative agent of treponemal diseases (Table S13). While *T. pallidum* is responsible for syphilis, other subspecies such as *T. p. endemicum* and *T. p. pertenue* cause bejel and yaws, respectively. Although today these diseases are geographically restricted to tropical regions,⁴⁸ previous genomic studies have confirmed the historical presence of diverse *Treponema* lineages, including non-syphilitic forms, in Finland.⁴⁹

We note that to confirm the presence of pathogens, and conclusively distinguish them from related species, pathogen capture would be required. Nevertheless, the screening results provide a glimpse into the variety of infections that could have afflicted medieval and historical populations of Pälkäne.

Personal traits and genetic predispositions

We used two tools, HlrisPlex⁵⁰ and Promethease (<https://promethease.com/>), to infer phenotypic traits and potential genetic predispositions of the individuals. For HlrisPlex, we used allele count data derived directly from the BAM files, and for Promethease, we used imputed data.

HlrisPlex analysis suggests that most of the individuals likely had blonde or dark blonde hair and blue eyes (Table S15), consistent with northern European populations in the medieval period.⁵¹ Two individuals (PKN002 and PLN002) likely had darker brown hair, whereas PKN006, an elderly male, may have had red hair. One child, PLN001, likely had brown eyes and black hair.

According to the Promethease reports (Table S16), the majority of the individuals (at least 6 out of 10) could digest milk to some extent. Lactase persistence is particularly high in Finland and other Nordic countries, with a prevalence exceeding 80% in present-day Finland.⁵² This high frequency is generally linked to the nutritional benefits of milk consumption in dairy-farming societies,^{53,54} although archaeological evidence shows that dairy products were consumed long before lactase persistence became widespread in Europe.^{54,55} Evershed et al.⁵⁵ have argued that milk might have been a critical but risky food source

for lactose intolerant individuals during times of famine and epidemic disease, thus driving natural selection in favor of lactase persistence. In Finland, dairy farming and milk consumption became increasingly common only in the 19th century CE,⁵⁶ suggesting that the high frequency of the allele in present-day Finnish population is not linked to milk consumption in Finland.

With respect to pathologies, PLN004 may have carried a genetic variant associated with an eye disease, Fuchs endothelial corneal dystrophy-6 (FECD) (Table S16). It is the most common genetic disorder affecting the corneal endothelium,⁵⁷ but it does not necessarily have a strong effect on the individual, as the symptoms vary from less severe eye pain to problems with eyesight. Promethase also reported various allele variants associated with disease risks for other individuals (Table S16). Although such reports have occasionally been used in ancient DNA research,^{58,59} their results require cautious interpretation due to the highly polygenic basis of most hereditary diseases, coupled with environmental effects on phenotypic expressions. We did not calculate polygenic risk scores for any of the traits due to their likely poor predictive power at the individual level. Low coverage and postmortem DNA damage, characteristic of ancient DNA, would add further uncertainty to any polygenic risk scores we might calculate.

Although the small sample size prevents robust analysis of disease-related traits, studies with larger datasets coupled with ancient pathogen findings could provide valuable insights into immune-related selection and the historical prevalence of infections in Finland. Moreover, information on the individual genetic traits can be used in popularization of archaeogenetics, for example, in museum exhibitions: it potentially adds an aspect of human interest and helps to depict the ancient individuals as more relatable people with individual traits.

Interdisciplinary insights into human past

Finland has long remained underrepresented in European ancient DNA research, primarily due to poor preservation of organic material in the acidic soils. This study offers a rare contribution by providing new information on the genetic composition, health, and kinship patterns of medieval Finnish populations. When integrated with archaeological evidence, the results also shed light on burial customs, the spread of Christianity, and regional social networks during a formative period in Finland's history. The relatively recent chronology of the analyzed individuals enabled the use of Finnish Biobank reference data, allowing for direct comparisons between ancient and modern populations. The results have also been used in a museum exhibition Ancient DNA: A Key to the Past (Museum Center Vapriikki, Finland), highlighting the value of interdisciplinary approach in sparking public interest for ancient individuals and their research.

Limitations of the study

This study provides insights into the genetic history, mobility, and health of medieval and post-medieval populations in the Pirkanmaa region of Finland. However, several limitations should be acknowledged. First, the small sample size, dictated by the scarcity of well-preserved skeletal remains in Finland's acidic soils, limits the statistical power of analyses. Our analyses

comparing the ancient individuals with present-day individuals from the Finnish Biobank could be affected by the sample selection of the original modern samples and data production. Sampling for the Finnish Biobank has heavily targeted the modern-day regions of North Karelia, North Savo, and Northern Ostrobothnia. Moreover, the Finnish Biobank data used in the IBD analyses in this study was produced by the Human Core Exome chip, which has limited overlap with the 1240k capture panel used in the aDNA data production. Limited number of markers likely reduces our power to detect IBD segments.

RESOURCE AVAILABILITY

Lead contact

Further information and requests for resources should be directed to and will be fulfilled by the lead contact, Ulla Nordfors (ulla.nordfors@utu.fi).

Materials availability

This study did not generate new unique reagents.

Data and code availability

- Raw sequencing data from the newly sequenced individuals have been deposited at European Nucleotide Archive (ENA) as ENA: PRJEB88970 and are publicly available as of the date of publication.
- Genotype data have been deposited at the Poseidon community archive and are publicly available as of the date of publication at: <https://github.com/poseidon-framework/community-archive>.
- This paper analyzes existing, publicly available genotype data, accessible at <https://github.com/poseidon-framework/community-archive>.
- This paper analyzes existing genotype data from THL Biobank, accessible via application procedure at www.thl.fi/biobank.
- This paper does not report original code.
- Any additional information required to reanalyze the data reported in this paper is available from the [lead contact](#) upon request.

ACKNOWLEDGMENTS

We are grateful to the Jena lab team at the MPI-EVA for carrying out laboratory work for the samples in this study. We would also like to thank Kay Prüfer, Alexander Herbig, and Harald Ringbauer for developing and running data processing and analysis pipelines at the MPI-EVA, as well as the Population Genetics group for helpful discussions.

We acknowledge the funding provided by the Human Diversity consortium, Profi7 program by the Research Council of Finland, grant 352727. The samples from Ristiänmäki and three samples from Rauniokirkko were part of the SUGRIGE project, funded by the Jane and Aatos Erkko Foundation. Museum Center Vapriikki funded the excavation at Rauniokirkko and the DNA analysis of recovered individuals. We also thank the Finnish Cultural Foundation for supporting S.P. and Museum Center Vapriikki for funding S.P. and U.N. Open Access funded by Helsinki University Library

The modern Finnish data used for the research were obtained from THL Biobank www.thl.fi/biobank (study number: BB2019_2). We thank all study participants for their generous participation at THL Biobank and the National FINRISK and Health 2000 studies.

AUTHOR CONTRIBUTIONS

Conceptualization, U.N.; methodology, S.P.; laboratory work, K.M.; bioinformatic processing, S.P., R.J.O.S., E.S., T.C.L., L.T., and A.A.V.; data analysis, S.P., U.N., R.J.O.S., T.C.L., L.T., and A.A.V.; data curation, S.P. and E.S.; investigation, U.N. and S.P.; writing—original draft, S.P. and U.N.; writing—review and editing, U.N., S.P., R.J.O.S., E.S., K.M., A.A.V., and P.O.; resources, U.N., J.K., and P.O.; visualization, S.P. and U.N.; supervision, E.S., P.O., J.K., and U.N.; project administration, U.N. and P.O.

DECLARATION OF INTERESTS

The authors declare no competing interests.

STAR★METHODS

Detailed methods are provided in the online version of this paper and include the following:

- **KEY RESOURCES TABLE**
- **EXPERIMENTAL MODEL AND STUDY PARTICIPANT DETAILS**
 - Subject details – The archaeological sites
- **METHOD DETAILS**
 - DNA extraction, library preparation, capture, and sequencing
- **QUANTIFICATION AND STATISTICAL ANALYSIS**
 - Bioinformatic processing
 - Imputation
 - Contamination estimation
 - Analysis of uniparentally-inherited markers
 - HapROH, kinship, and ancIBD
 - Reference datasets
 - PCA
 - ADMIXTURE
 - F statistics
 - IBD connectivity and spatial interpolation
 - Promethease and HlrisPlex
 - Pathogen screening

SUPPLEMENTAL INFORMATION

Supplemental information can be found online at <https://doi.org/10.1016/j.isci.2025.113086>.

Received: May 4, 2025

Revised: June 16, 2025

Accepted: July 7, 2025

Published: July 9, 2025

REFERENCES

1. Moilanen, U. (2021). Variations in inhumation burial customs in southern Finland (AD 900–1400): Case studies from Häme and Upper Satakunta. University of Turku., 152659. <https://www.utupub.fi/handle/10024/>.
2. Pitkänen, K. (2007). Suomen väestön historialliset kehityslinjat. In M. Rynnänen, I. Söderling, S. Suomen väestö, S. Koskinen, T. Martelin, I.-L. Notkola, V. Notkola, K. Pitkänen, M. Jalovaara, E. Mäenpää, and A. Ruokolainen, eds. (Gaudeamus Helsinki University Press), pp. 41–76.
3. Raninen S., Wessman A. Rautakausi. In: Haggrén G., Halinen P., Lavento M., Raninen S., Wessman A., editors. Muinaisuutemme jäljet: Suomen esija varhaishistoria kivikaudelta keskiajalle; 2015. p. 215–365. Gaudeamus
4. Keränen J. Kainuun asuttaminen. *Studia historica Jyväskylälänsia*, University of Jyväskylä. <https://jyx.jyu.fi/handle/123456789/75370>; 1984.
5. Aikio, Å. (2012). An essay on Saami ethnolinguistic prehistory. *Suomalais-Ugrilaisen Seuran Toimituksia = Mémoires de la Société Finno-Ougrienne* 266, 63–117.
6. de la Chapelle, A., and Wright, F.A. (1998). Linkage disequilibrium mapping in isolated populations: the example of Finland revisited. *Proc. Natl. Acad. Sci. USA* 95, 12416–12423.
7. Varilo, T., Laan, M., Hovatta, I., Wiebe, V., Terwilliger, J.D., and Peltonen, L. (2000). Linkage disequilibrium in isolated populations: Finland and a young sub-population of Kuusamo. *Eur. J. Hum. Genet.* 8, 604–612.
8. Kerminen, S., Cerioli, N., Pacauskas, D., Havulinna, A.S., Perola, M., Jousilahti, P., Salomaa, V., Daly, M.J., Vyas, R., Ripatti, S., and Pirinen, M. (2021). Changes in the fine-scale genetic structure of Finland through the 20th century. *PLoS Genet.* 17, e1009347.
9. Borodulin, K., Tolonen, H., Jousilahti, P., Jula, A., Juolevi, A., Koskinen, S., Kuulasmaa, K., Laatikainen, T., Männistö, S., Peltonen, M., et al. (2018). Cohort profile: The national FINRISK study. *Int. J. Epidemiol.* 47, 696–696i.
10. Kirkinen, H. (1970). Karjala idän ja lännen välissä. I, Venäjän Karjala renessanssiajalla (1478-1617). Kirjayhtymä. <https://www.doria.fi/handle/10024/170166>.
11. Voutilainen, M., Helse, J., and Högmänder, H. (2020). A Bayesian reconstruction of a historical population in Finland, 1647–1850. *Demography* 57, 1171–1192.
12. Eriksen, A.M.H., Rodriguez, J.A., Seersholm, F., Hollund, H.I., Gotfredsen, A.B., Collins, M.J., Grønnow, B., Pedersen, M.W., Gilbert, M.T.P., and Matthiesen, H. (2025). Exploring DNA degradation *in situ* and in museum storage through genomics and metagenomics. *Commun. Biol.* 8, 210.
13. Alexander, D.H., Novembre, J., and Lange, K. (2009). Fast model-based estimation of ancestry in unrelated individuals. *Genome Res.* 19, 1655–1664.
14. Fu, Q., Mittnik, A., Johnson, P.L.F., Bos, K., Lari, M., Bollongino, R., Sun, C., Giemsch, L., Schmitz, R., Burger, J., et al. (2013). A Revised Timescale for Human Evolution Based on Ancient Mitochondrial Genomes. *Curr. Biol.* 23, 553–559.
15. Renaud, G., Slon, V., Duggan, A.T., and Kelso, J. (2015). Schmutzi: Estimation of contamination and endogenous mitochondrial consensus calling for ancient DNA. *Genome Biol.* 16, 224.
16. O'Connor, T.D., Fu, W., NHLBI GO Exome Sequencing Project, ESP Population Genetics and Statistical Analysis Working Group Emily Turner, Mychaleckyj, J.C., Logsdon, B., Auer, P., Carlson, C.S., Leal, S.M., Smith, J. D., et al. (2015). Rare variation facilitates inferences of fine-scale population structure in humans. *Mol. Biol. Evol.* 32, 653–660.
17. Alaçamlı, E., Naidoo, T., Güler, M.N., Sağlıcan, E., Aktürk, Ş., Mapelli, I., Vural, K.B., Somel, M., Malmström, H., and Günther, T. (2024). READv2: advanced and user-friendly detection of biological relatedness in archaeogenomics. *Genome Biol.* 25, 216.
18. Moilanen, U. (2023). Ruumishautojen ajoittamisen haasteellisuus: Tapausesimerkinä Pälkäneen rauniokirkko. *Muinaistutkija*, 19–35. <https://muinaistutkija.journal.fi/article/view/128729>.
19. Meyer, C., Ganslmeier, R., Dresely, V., and Alt, K.W. (2012). New approaches to the reconstruction of kinship and social structure based on bioarchaeological analysis of Neolithic multiple and collective graves. *Theoretical and methodological considerations in Central European Neolithic archaeology* 2325, 11–23.
20. Murphy, E., and Donnelly, C. (2018). Together in death: Demography and funerary practices in contemporary multiple internments in Irish medieval burial grounds (AmS-skrifter), pp. 119–142.
21. Taavitsainen, J.-P. (2005). Finland in the middle ages. *Archaeol. J.* 162, 11–17.
22. Hiekkänen, M. (2010). Burial Practices in Finland. In *Från hedniskt till Kristet. Förändringar i begravningsbruk och gravskick i Sverige c:a 800–1200*, B. Nilsson, ed., pp. 271–379. Sällskapet Runica et Mediævalia.
23. Barbiera, I. (2015). Buried Together, Buried Alone: Christian Commemoration and Kinship in the Early Middle Ages. *Early Mediev. Eur.* 23, 385–409.
24. Ringbauer, H., Huang, Y., Akbari, A., Mallick, S., Olalde, I., Patterson, N., and Reich, D. (2024). Accurate detection of identity-by-descent segments in human ancient DNA. *Nat. Genet.* 56, 143–151.
25. Ringbauer, H., Novembre, J., and Steinrücken, M. (2021). Parental relatedness through time revealed by runs of homozygosity in ancient DNA. *Nat. Commun.* 12, 1–11.
26. Martin, A.R., Karczewski, K.J., Kerminen, S., Kurki, M.I., Sarin, A.P., Artomov, M., Eriksson, J.G., Esko, T., Genovese, G., Havulinna, A.S., et al. (2018). Haplotype sharing provides insights into fine-scale population history and disease in Finland. *Am. J. Hum. Genet.* 102, 760–775.
27. Jorde, L.B., and Pitkänen, K.J. (1991). Inbreeding in Finland. *Am. J. Phys. Anthropol.* 84, 127–139.

28. Gustin I. Contacts, identity, and hybridity: Objects from South-western Finland in the Birka graves. Callmer, J., Gustin, I., Roslund, M., editors. *Identity Formation and Diversity in the Early Medieval Baltic and Beyond*. Brill; 2017. p. 205–258.
29. Suvanto, S. (1973). *Satakunnan historia III. Keskiäika.. Satakunnan maakuntaliitto* <https://digi.kirjastot.fi/items/show/124721>.
30. Ralf, A., Montiel González, D., Zhong, K., and Kayser, M. (2018). Yleaf: Software for Human Y-Chromosomal Haplogroup Inference from Next-Generation Sequencing Data. *Mol. Biol. Evol.* 35, 1291–1294.
31. Rootsi, S., Magri, C., Kivisild, T., Benuzzi, G., Help, H., Bermisheva, M., Kutuev, I., Barac, L., Pericic, M., Balanovsky, O., et al. (2004). Phylogeography of Y-chromosome haplogroup I reveals distinct domains of prehistoric gene flow in Europe. *Am. J. Hum. Genet.* 75, 128–137.
32. Preussner, A., Leinonen, J., Riikonen, J., Pirinen, M., and Tukiainen, T. (2025). Y chromosome sequencing data suggest dual paths of haplogroup N1a1 into Finland. *Eur. J. Hum. Genet.* 33, 89–97.
33. Margaryan, A., Lawson, D.J., Sikora, M., Racimo, F., Rasmussen, S., Moltke, I., Cassidy, L.M., Jørsboe, E., Ingason, A., Pedersen, M.W., et al. (2020). Population genomics of the Viking world. *Nature* 585, 390–396.
34. Krzewińska, M., Kjellström, A., Günther, T., Hedenstierna-Jonson, C., Zachrisson, T., Omrak, A., Yaka, R., Kilinç, G.M., Somel, M., Sobrado, V., et al. (2018). Genomic and Strontium Isotope Variation Reveal Immigration Patterns in a Viking Age Town. *Curr. Biol.* 28, 2730–2738.e10.
35. Rodríguez-Varela, R., Moore, K.H.S., Ebenesersdóttir, S.S., Kilinc, G.M., Kjellström, A., Pappmehl-Dufay, L., Alfsdotter, C., Berglund, B., Alrawi, L., Kashuba, N., et al. (2023). The genetic history of Scandinavia from the Roman Iron Age to the present. *Cell* 186, 32–46.e19.
36. Speidel, L., Silva, M., Booth, T., Raffield, B., Anastasiadou, K., Barrington, C., Götherström, A., Heather, P., and Skoglund, P. (2025). High-resolution genomic history of early medieval Europe. *Nature* 637, 118–126.
37. Lamnidis, T.C., Majander, K., Jeong, C., Salmela, E., Wessman, A., Moiseyev, V., Khartanovich, V., Balanovsky, O., Ongyerth, M., Weihmann, A., et al. (2018). Ancient Fennoscandian genomes reveal origin and spread of Siberian ancestry in Europe. *Nat. Commun.* 9, 5018.
38. Tambets, K., Yunusbayev, B., Hudjashov, G., Ilumäe, A.M., Rootsi, S., Honkola, T., Vesakoski, O., Atkinson, Q., Skoglund, P., Kushniarevich, A., et al. (2018). Genes reveal traces of common recent demographic history for most of the Uralic-speaking populations. *Genome Biol.* 19, 139.
39. Jeong, C., Balanovsky, O., Lukianova, E., Kahbatkyzy, N., Flegontov, P., Zaporozhchenko, V., Immel, A., Wang, C.C., Ixan, O., Khussainova, E., et al. (2019). The genetic history of admixture across inner Eurasia. *Nat. Ecol. Evol.* 3, 966–976.
40. Hübler, R., Key, F.M., Warinner, C., Bos, K.I., Krause, J., and Herbig, A. (2019). HOPS: automated detection and authentication of pathogen DNA in archaeological remains. *Genome Biol.* 20, 280.
41. Fellows Yates, J.A., Lamnidis, T.C., Borry, M., Andrades Valtueña, A., Fagernäs, Z., Clayton, S., Garcia, M.U., Neukamm, J., and Peltzer, A. (2021). Reproducible, portable, and efficient ancient genome reconstruction with *nfcore/eager*. *PeerJ* 9, e10947.
42. Andrades Valtueña, A., Mittnik, A., Key, F.M., Haak, W., Allmäe, R., Belinskij, A., Daubaras, M., Feldman, M., Jankauskas, R., Janković, I., et al. (2017). The stone age plague and its persistence in Eurasia. *Curr. Biol.* 27, 3683–3691.e8.
43. Kallioinen, M. (1998). Pestepidemierna och bosättningsexpansionen i det medeltida Finland (Historisk Tidskrift för Finland). <https://journal.fi/htf/article/view/52988>.
44. Brady, M.F., Yarrarapu, S.N.S., and Anjum, F. (2024). *Yersinia Pseudotuberculosis*. In *StatPearls* (StatPearls Publishing). <http://www.ncbi.nlm.nih.gov/books/NBK430717/>.
45. Yue, Y., Zheng, J., Sheng, M., Liu, X., Hao, Q., Zhang, S., Xu, S., Liu, Z., Hou, X., Jing, H., et al. (2023). Public Health Implications of *Yersinia Enterocolitica* Investigation: An Ecological Modeling and Molecular Epidemiology Study. *Infect. Dis. Poverty* 12, 41.
46. Ramesh A., Padmapriya B.P., Bharathi S., Varadaraj M.C. *YERSINIA ENTEROCOLITICA | Detection and Treatment*. Caballero, B., Finglas, P., Toldra, F., editors. *Encyclopedia of Food Sciences and Nutrition*. Elsevier; 2003. p. 6245–6252.
47. Roupheal, N.G., and Stephens, D.S. (2012). *Neisseria meningitidis: Biology, Microbiology, and Epidemiology*. In *Neisseria meningitidis: Advanced Methods and Protocols*, M. Christodoulides, ed. (Humana Press), pp. 1–20.
48. Giacani, L., and Lukehart, S.A. (2014). The endemic treponematoses. *Clin. Microbiol. Rev.* 27, 89–115.
49. Majander, K., Pfrengle, S., Kocher, A., Neukamm, J., du Plessis, L., Pla-Díaz, M., Arora, N., Akgül, G., Salo, K., Schats, R., et al. (2020). Ancient bacterial genomes reveal a high diversity of *Treponema pallidum* strains in early modern Europe. *Curr. Biol.* 30, 3788–3803.e10.
50. Walsh, S., Chaitanya, L., Clarisse, L., Wirken, L., Draus-Barini, J., Kovatsi, L., Maeda, H., Ishikawa, T., Sijen, T., de Knijff, P., et al. (2014). Developmental validation of the HirisPlex system: DNA-based eye and hair colour prediction for forensic and anthropological usage. *Forensic Sci. Int. Genet.* 9, 150–161.
51. Draus-Barini, J., Walsh, S., Pošpiech, E., Kupiec, T., Głab, H., Branicki, W., and Kayser, M. (2013). Bona fide colour: DNA prediction of human eye and hair colour from ancient and contemporary skeletal remains. *Invest. Genet.* 4, 3.
52. Storhaug, C.L., Fosse, S.K., and Fadnes, L.T. (2017). Country, regional, and global estimates for lactose malabsorption in adults: a systematic review and meta-analysis. *Lancet Gastroenterol. Hepatol.* 2, 738–746.
53. Leonardi, M., Gerbault, P., Thomas, M.G., and Burger, J. (2012). The evolution of lactase persistence in Europe. A synthesis of archaeological and genetic evidence. *Int. Dairy J.* 22, 88–97.
54. Burger, J., Link, V., Blöcher, J., Schulz, A., Sell, C., Pochon, Z., Diekmann, Y., Žegarac, A., Hofmanová, Z., Winkelbach, L., et al. (2020). Low prevalence of lactase persistence in Bronze Age Europe indicates ongoing strong selection over the last 3,000 years. *Curr. Biol.* 30, 4307–4315.e13.
55. Evershed, R.P., Davey Smith, G., Roffet-Salque, M., Timpson, A., Diekmann, Y., Lyon, M.S., Cramp, L.J.E., Casanova, E., Smyth, J., Whelton, H.L., et al. (2022). Dairying, diseases and the evolution of lactase persistence in Europe. *Nature* 608, 336–345.
56. Vihola, T. (1991). Leipävlijasta lypsytarjaan: maatalouden tuotantosuunnan muutos Suomessa 1870-luvulta ensimmäisen maailmansodan vuosiin. Suomen historiallinen seura.
57. Vedana, G., Villarreal, G., Jr., and Jun, A.S. (2016). Fuchs endothelial corneal dystrophy: current perspectives (Clinical ophthalmology), pp. 321–330.
58. Peltzer, A., Mittnik, A., Wang, C.-C., Begg, T., Posth, C., Nieselt, K., and Krause, J. (2018). Inferring genetic origins and phenotypic traits of George Bähr, the architect of the Dresden Frauenkirche. *Sci. Rep.* 8, 2115.
59. Du, P., Zhu, K., Qiao, H., Zhang, J., Meng, H., Huang, Z., Yu, Y., Xie, S., Allen, E., Xiong, J., et al. (2024). Ancient genome of the Chinese Emperor Wu of Northern Zhou. *Curr. Biol.* 34, 1587–1595.e5.
60. Renaud, G., Stenzel, U., and Kelso, J. (2014). *leeHom*: adaptor trimming and merging for Illumina sequencing reads. *Nucleic Acids Res.* 42, e141.
61. Li, H., Handsaker, B., Wysoker, A., Fennell, T., Ruan, J., Homer, N., Marth, G., Abecasis, G., and Durbin, R.; 1000 Genome Project Data Processing Subgroup (2009). The Sequence Alignment/Map format and SAMtools. *Bioinformatics* 25, 2078–2079.
62. Link, V., Kousathanas, A., Veeramah, K., Sell, C., Scheu, A., and Wegmann, D. (2017). ATLAS: Analysis Tools for Low-depth and Ancient Samples. Preprint at bioRxiv. <https://doi.org/10.1101/105346>.
63. Rubinacci, S., Ribeiro, D.M., Hofmeister, R.J., and Delaneau, O. (2021). Efficient phasing and imputation of low-coverage sequencing data using large reference panels. *Nat. Genet.* 53, 120–126.

64. Jónsson, H., Ginolhac, A., Schubert, M., Johnson, P.L.F., and Orlando, L. (2013). mapDamage2.0: fast approximate Bayesian estimates of ancient DNA damage parameters. *Bioinformatics* 29, 1682–1684.
65. Korneliusen, T.S., Albrechtsen, A., and Nielsen, R. (2014). ANGSD: Analysis of Next Generation Sequencing Data. *BMC Bioinf.* 15, 356.
66. Schönherr, S., Weissensteiner, H., Kronenberg, F., and Forer, L. (2023). Haplogrep 3 - an interactive haplogroup classification and analysis platform. *Nucleic Acids Res.* 51, W263–W268.
67. Shannon, P., Markiel, A., Ozier, O., Baliga, N.S., Wang, J.T., Ramage, D., Amin, N., Schwikowski, B., and Ideker, T. (2003). Cytoscape: a software environment for integrated models of biomolecular interaction networks. *Genome Res.* 13, 2498–2504.
68. Schmid, C., Ghalichi, A., Lamnidis, T.C., Mudiyansele, D.B.A., Haak, W., and Schiffels, S. (2024). Poseidon – A framework for archaeogenetic human genotype data management. <https://doi.org/10.7554/elife.98317.1>.
69. Purcell, S., Neale, B., Todd-Brown, K., Thomas, L., Ferreira, M.A.R., Bender, D., Maller, J., Sklar, P., de Bakker, P.I.W., Daly, M.J., and Sham, P.C. (2007). PLINK: a tool set for whole-genome association and population-based linkage analyses. *Am. J. Hum. Genet.* 81, 559–575.
70. Manichaikul, A., Mychaleckyj, J.C., Rich, S.S., Daly, K., Sale, M., and Chen, W.-M. (2010). Robust relationship inference in genome-wide association studies. *Bioinformatics* 26, 2867–2873.
71. Patterson, N., Price, A.L., and Reich, D. (2006). Population structure and eigenanalysis. *PLoS Genet.* 2, e190–e2093.
72. Seidman, D.N., Shenoy, S.A., Kim, M., Babu, R., Woods, I.G., Dyer, T.D., Lehman, D.M., Curran, J.E., Duggirala, R., Blangero, J., and Williams, A.L. (2020). Rapid, Phase-free Detection of Long Identity-by-Descent Segments Enables Effective Relationship Classification. *Am. J. Hum. Genet.* 106, 453–466.
73. Vågene, Å.J., Herbig, A., Campana, M.G., Robles García, N.M., Warinner, C., Sabin, S., Spyrou, M.A., Andrades Valtueña, A., Huson, D., Tuross, N., et al. (2018). Salmonella enterica genomes from victims of a major sixteenth-century epidemic in Mexico. *Nat. Ecol. Evol.* 2, 520–528.
74. Tiilikkala, J. (2023). Kangasala Vehoniemenharju 4 Rautakautisen ja keskiaikaisen kulkuväylien tarkastus 2023 (Archives of Finnish Heritage Agency).
75. Orfanou, E., Himmel, M., Aron, F., and Haak, W. (2020). Minimally-invasive sampling of pars petrosa (os temporale) for ancient DNA extraction. [protocols.io](https://doi.org/10.17504/protocols.io.bqd8ms9w).
76. Neumann, G., Valtuena, A.A., Yates, J.F., Stahl, R., and Brandt, G. (2020). Tooth Sampling from the inner pulp chamber for ancient DNA Extraction. [protocols.io](https://doi.org/10.17504/protocols.io.bqd8ms9w). <https://doi.org/10.17504/protocols.io.bqd8ms9w>.
77. Dabney, J., Knapp, M., Glocke, I., Gansauge, M.-T., Weihmann, A., Nickel, B., Valdiosera, C., García, N., Pääbo, S., Arsuaga, J.-L., and Meyer, M. (2013). Complete mitochondrial genome sequence of a Middle Pleistocene cave bear reconstructed from ultrashort DNA fragments. *Proc. Natl. Acad. Sci. USA* 110, 15758–15763.
78. Rohland, N., Glocke, I., Aximu-Petri, A., and Meyer, M. (2018). Extraction of highly degraded DNA from ancient bones, teeth and sediments for high-throughput sequencing. *Nat. Protoc.* 13, 2447–2461.
79. Velsko, I., Skouranioti, E., and Brandt, G. (2020). Ancient DNA Extraction from Skeletal Material. [protocols.io](https://doi.org/10.17504/protocols.io.baksicw). <https://doi.org/10.17504/protocols.io.baksicw>.
80. Gansauge, M.T., Gerber, T., Glocke, I., Korlević, P., Lippik, L., Nagel, S., Riehl, L.M., Schmidt, A., and Meyer, M. (2017). Single-stranded DNA library preparation from highly degraded DNA using T4 DNA ligase. *Nucleic Acids Res.* 45, e79.
81. Gansauge, M.-T., Aximu-Petri, A., Nagel, S., and Meyer, M. (2020). Manual and automated preparation of single-stranded DNA libraries for the sequencing of DNA from ancient biological remains and other sources of highly degraded DNA. *Nat. Protoc.* 15, 2279–2300.
82. Mathieson, I., Lazaridis, I., Rohland, N., Mallick, S., Patterson, N., Roodenberg, S.A., Harney, E., Stewardson, K., Fernandes, D., Novak, M., et al. (2015). Genome-wide patterns of selection in 230 ancient Eurasians. *Nature* 528, 499–503.
83. Fu, Q., Meyer, M., Gao, X., Stenzel, U., Burbano, H.a., Kelso, J., and Pääbo, S. (2013). DNA analysis of an early modern human from Tianyuan Cave, China. *Proc. Natl. Acad. Sci. USA* 110, 2223–2227.
84. Meyer, M., and Kircher, M. (2010). Illumina sequencing library preparation for highly multiplexed target capture and sequencing. *Cold Spring Harb. Protoc.* 2010, pdb.prot5448.
85. Rohland, N., Harney, E., Mallick, S., Nordenfelt, S., and Reich, D. (2015). Partial uracil – DNA – glycosylase treatment for screening of ancient DNA. *Philos. Trans. R. Soc. Lond. B Biol. Sci.* 370, 20130624. <https://doi.org/10.1098/rstb.2013.0624>.
86. Li, H., and Durbin, R. (2010). Fast and accurate long-read alignment with Burrows-Wheeler transform. *Bioinformatics* 26, 589–595.
87. 1000 Genomes Project Consortium; Auton, A., Brooks, L.D., Durbin, R.M., Garrison, E.P., Kang, H.M., Korbel, J.O., Marchini, J.L., McCarthy, S., McVean, G.A., and Abecasis, G.R. (2015). A global reference for human genetic variation. *Nature* 526, 68–74.
88. Lazaridis, I., Patterson, N., Mittnik, A., Renaud, G., Mallick, S., Kirsanow, K., Sudmant, P.H., Schraiber, J.G., Castellano, S., Lipson, M., et al. (2014). Ancient human genomes suggest three ancestral populations for present-day Europeans. *Nature* 513, 409–413.
89. Mallick, S., Li, H., Lipson, M., Mathieson, I., Gymrek, M., Racimo, F., Zhao, M., Chennagiri, N., Nordenfelt, S., Tandon, A., et al. (2016). The Simons Genome Diversity Project: 300 genomes from 142 diverse populations. *Nature* 538, 201–206.
90. Pebesma, E.J. (2004). Multivariable geostatistics in S: the gstat package. *Comput. Geosci.* 30, 683–691.
91. Cariaso, M., and Lennon, G. (2012). SNPedia: a wiki supporting personal genome annotation, interpretation and analysis. *Nucleic Acids Res.* 40, D1308–D1312.
92. Schubert, M., Lindgreen, S., and Orlando, L. (2016). AdapterRemoval v2: rapid adapter trimming, identification, and read merging. *BMC Res. Notes* 9, 88.
93. Herbig, A., Maixner, F., Bos, K.I., Zink, A., Krause, J., and Huson, D.H. (2016). MALT: Fast alignment and analysis of metagenomic DNA sequence data applied to the Tyrolean Iceman. Preprint at bioRxiv. <https://doi.org/10.1101/50559>.

STAR★METHODS

KEY RESOURCES TABLE

REAGENT or RESOURCE	SOURCE	IDENTIFIER
Biological samples		
Ancient skeletal element	Finnish Heritage Agency	KM44296:1
Ancient skeletal element	Finnish Heritage Agency	KM44296:2
Ancient skeletal element	Finnish Heritage Agency	KM44296:4
Ancient skeletal element	Finnish Heritage Agency	KM44296:6
Ancient skeletal element	Finnish Heritage Agency	KM44296:7
Ancient skeletal element	Finnish Heritage Agency	KM44296:8
Ancient skeletal element	Finnish Heritage Agency	KM44296:12
Ancient skeletal element	Finnish Heritage Agency	KM44296:10
Ancient skeletal element	Finnish Heritage Agency	KM44296:9
Ancient skeletal element	Finnish Heritage Agency	KM44296:13
Ancient skeletal element	Finnish Heritage Agency	KM44296:14
Ancient skeletal element	Finnish Heritage Agency	KM44296:22
Ancient skeletal element	Finnish Heritage Agency	KM44296:23
Ancient skeletal element	Finnish Heritage Agency	KM44296:27
Ancient skeletal element	Finnish Heritage Agency	KM2004045:237
Ancient skeletal element	Finnish Heritage Agency	KM2004045:238
Ancient skeletal element	Finnish Heritage Agency	KM2004045:207
Ancient skeletal element	Finnish Heritage Agency	KM22081: 55
Ancient skeletal element	Finnish Heritage Agency	KM22081: 42
Ancient skeletal element	Finnish Heritage Agency	KM22081: 32
Ancient skeletal element	Finnish Heritage Agency	KM22081: 19
Ancient skeletal element	Finnish Heritage Agency	KM17208:129
Ancient skeletal element	Finnish Heritage Agency	KM17208:466
Ancient skeletal element	Finnish Heritage Agency	KM17208:271
Ancient skeletal element	Vapriikki Museum Center	HM3064:5
Deposited data		
BAM	This study	ENA:PRJEB88970
Genotypes	This study	Poseidon community archive
Software and algorithms		
leeHom v1.1.5	Renaud, Stenzel, and Kelso ⁶⁰	https://github.com/grenaud/leeHom
BWA v0.7.12	Li and Durbin ⁶¹	https://github.com/lh3/bwa
nf-core/eager v2.5.0	Fellows Yates et al. ⁴¹	https://github.com/nf-core/eager/
picard MarkDuplicates v2.26.0	N/A	https://broadinstitute.github.io/picard/
SequenceTools v1.5.2	N/A	https://github.com/stschiff/sequenceTools
Sex.DetERRmine	Lamnidis et al. ³⁷	https://github.com/TCLamnidis/Sex.DetERRmine
Samtools v1.12	Li et al. 2009 ⁶¹	https://github.com/samtools/samtools
ATLAS	Link et al. ⁶²	N/A
GLIMPSE	Rubinacci et al. ⁶³	https://github.com/odelaneau/GLIMPSE
MapDamage2 v2.2.1	Jónsson et al. ⁶⁴	https://github.com/ginolhac/mapDamage
contamMix	Fu et al. ¹⁴	N/A
Schmutzi	Renaud et al. ¹⁵	https://github.com/grenaud/schmutzi
ANGSD	Korneliussen, Albrechtsen, and Nielsen ⁶⁵	https://github.com/ANGSD/angsd
Haplogrep3	Schönherr et al. ⁶⁶	https://github.com/genepi/haplogrep3

(Continued on next page)

Continued

REAGENT or RESOURCE	SOURCE	IDENTIFIER
Yleaf	Ralf et al. ³⁰	https://github.com/genid/Yleaf
hapROH	Ringbauer, Novembre, and Steinrücken ²⁵	https://haproh.readthedocs.io/en/latest
READv2	Alaçamlı et al. ¹⁷	https://github.com/GuntherLab/READv2
ancIBD	Ringbauer et al. ²⁴	https://ancibd.readthedocs.io/en/latest/
Cytoscape	Shannon et al. ⁶⁷	https://cytoscape.org/
trident	Schmid et al. ⁶⁸	https://www.poseidon-adna.org/
PLINK v1.90b3.29	Purcell et al. ⁶⁹	https://www.cog-genomics.org/plink/1.9/
KING	Manichaikul et al. ⁷⁰	https://www.kingrelatedness.com/
smartpca	Patterson, Price, and Reich ⁷¹	https://github.com/chrchang/eigensoft
ADMIXTURE	Alexander et al. ¹³	https://dalexander.github.io/admixture/
xerxes	Schmid et al. ⁶⁸	https://www.poseidon-adna.org/
IBIS	Seidman et al. ⁷²	https://github.com/williamslab/ibis
Promethase	N/A	https://promethase.com/
Hirisplex	Walsh et al. ⁵⁰	https://hirisplex.erasmusmc.nl/
MALT	Vågane et al. ⁷³	https://github.com/husonlab/malt
HOPS	Hübler et al. ⁴⁰	https://github.com/rhuebler/HOPS

EXPERIMENTAL MODEL AND STUDY PARTICIPANT DETAILS

Subject details – The archaeological sites

The three cemeteries – Tampere Vilusenharju, Pälkäne Rauniokirkko, and Pälkäne Ristiänmäki – offer a glimpse into burial practices and societal transitions in Early Medieval Finland, particularly the shift from cremation to inhumation around 11th–12th centuries CE. Vilusenharju is the only known Early Medieval inhumation cemetery in what is now the city of Tampere. The site was used for cremations in the 11th–12th centuries, but by the 12th century, inhumation burials began to appear alongside cremations, and burials continued until the 13th century. The site contains around 50 inhumations, and it is thought to have been associated with a small Christian settlement, possibly a farm or small village. The site suffered significant damage due to sand extraction in 1961, and only a portion of the cemetery was excavated in 1961 and 1962.¹ Only 4 of the 50 graves contained sufficient bone material for aDNA analysis. All sampled individuals (TMP001, TMP002, TMP003, and TMP004) date to the 13th century.

Rauniokirkko is located at the now-ruined St. Michael’s Church in Pälkäne, where burials took place from the 13th century until the early 19th century. The ruined church was built between 1495–1505, but there was a chapel located at the site from at least the 14th century onwards.²² It remains unclear whether the earliest burials dating to the 13th century are connected to a church. This site acts as a timeline of inhumation traditions in the region. Excavations at Rauniokirkko have been conducted in the 1990s, 2000s, and most recently in 2022, when 17 graves were excavated. The excavation in 2022 yielded an unusually high number of preserved remains, with 14 of 17 graves being suitable for genetic analysis. Seven individuals (PKN002, PKN003, PKN004, PKN005, PKN006, PKN008, PKN009) have been radiocarbon dated to the 13th century, two (PKN001 and PKN010) to the 16th century, one (PKN007) to the 17th century, and four (PKN011, PKN012, PKN013, PKN014) to the late 18th and early 19th centuries.¹⁸ For analytical purposes, this study categorizes the 15 individuals from the 13th-century Vilusenharju and Ristiänmäki as the medieval cluster and the remaining 7 from Rauniokirkko as the post-medieval cluster. Although the sample size is small, this temporal segmentation allows for a comparative analysis of these medieval and post-medieval individuals.

Ristiänmäki lies 1 km from Rauniokirkko, with 12 burials excavated between 1934 and 1983. Only 4 of these burials could be sampled: PLN001, PLN002, PLN003, PLN004. The cemetery was used between the 11th and 13th centuries, but the relationship between Ristiänmäki and Rauniokirkko remains unclear. It is not known whether the use of Ristiänmäki ceased when burials began at Rauniokirkko or if the two sites were used concurrently during the 13th century. The proximity of the two sites raises questions about continuity and change in local burial practices during the shift from pre-Christian to Christian customs.

These three cemeteries, located 30 km apart, are connected by a natural sandy esker (Figure 1), which served as a road from at least the 11th century CE.⁷⁴ This geographic link, along with the cemeteries’ chronological overlap, suggests possible connections between the communities associated with these burial sites.

METHOD DETAILS

DNA extraction, library preparation, capture, and sequencing

For the samples labelled PKN, TMP, and PLN, DNA extraction, and library preparation were carried out in the ancient DNA laboratory facility at the Max Planck Institute for Geoanthropology (formerly Max Planck Institute for the Science of Human History (MPI-SHH)),

Jena, and sequenced in the Max Planck Institute for Evolutionary Anthropology (MPI-EVA), Leipzig. We drilled approximately 50 mg of bone powder from the samples, following the procedures described in detail in Orfanou et al.⁷⁵ and Neumann et al.⁷⁶ Lysates were prepared in 2.0-ml Eppendorf Lo-Bind tubes following a method optimised for the recovery of short DNA fragments.^{77–79} We used between 30–53 mg of bone powder, or 0.8 mg of calculus, and 1.25 μ l of extraction buffer (0.45 M EDTA, 0.25 mg/ml proteinase K, 0.05% Tween-20) to prepare lysates. The lysates were incubated on rotation in 37°C for approximately 16 hours. DNA was extracted using an automated liquid handling system (Bravo NGS Workstation B, Agilent Technologies). DNA was purified from 150 μ l lysate using silica-coated magnetic beads and binding buffer D.⁷⁸

DNA extracts were converted to single-stranded DNA libraries using an automated protocol.^{80,81} Libraries were prepared from 30 ml of extract, and library yield and efficiency were determined with quantitative PCR assays. The libraries were amplified and each library was tagged with a unique pair of indices using AccuPrime Pfx DNA polymerase.

Libraries were sequenced to 5 million reads on Illumina HiSeq 4000 using 75 single-end cycles to screen their DNA preservation. Samples that had $\geq 0.1\%$ of sequences of ≥ 30 base pairs (bp) in length mapping to the human genome were further enriched for human DNA with in-solution hybridization capture using capture probes that target approximately 1.2 million genome-wide ancestry-informative markers.^{82,83} The enriched libraries were then sequenced to approximately 20 million reads with the same platform and setup as above. Additionally, one library (PKN004) was resequenced on Illumina NovaSeq X with 100 paired-end cycles.

For three samples excavated from Pälkäne Rauniokirkko in 2003, sampling was performed as described above, but the extraction was done following the manual version of the protocol described in Dabney et al.⁷⁷ The library preparation was also done manually, following a double-stranded protocol described by Meyer and Kircher.⁸⁴ These libraries were exposed to a partial uracil-N-glycosylase treatment to reduce the levels of DNA damage.⁸⁵ The libraries were enriched as described above, and sequenced to approximately 20 million reads on Illumina HiSeq 4000 with 75 single-end cycles. PLK003 was resequenced on the same platform with 50 paired-end cycles. For JK2285/PLK001 and JK2289/PLK005, laboratory work was carried out in the ancient DNA facilities at the University of Tübingen, and for JK2287/PLK003 in MPI-SHH.

Interestingly, we noted that bones appearing to be well-preserved upon visual inspection did not always yield viable DNA data, while poorly preserved bones could provide better results (Figure S1). Additionally, there was no clear correlation between the age of the samples and the success of the DNA retrieval, as some samples from the 13th century produced more data than those dating to the early 19th century (see Data S1).

QUANTIFICATION AND STATISTICAL ANALYSIS

Bioinformatic processing

Adapter sequences were trimmed using leeHom⁶⁰ 1.1.5 and parameters `-ancientdna`. Additional parameters were used for the paired-end sequencing data: `-f 'AGATCGGAAGAGCACACGTCTGAACTCCAGTCACIIIIIIATCTCGTATGCCGTCTTCTGCTTG'`, `-s 'GGAAGAGCGTCTGTAGGAAAGAGTGTAGATCTCGGTGGTCGCCGTATCATT'`, `-c 'ACACTCTTTCCCTACACGCTCTGAACTCCAG,ACACTCTTTCCCACACGTCTGAACTCCAGT,ACACTCTTTCCCTACACACGTCTGAACTCC,CTCTTTCCCTACACGTCTGAACTCCA GTCA,GAAGAGCACACGTCTGAACTCCAGTCACII,GAGCACACGTCTGAACTCCAGTCACIIII,GATCGGAAGAGCACACGTCTGAAC TCCAGT,AGATCGGAAGAGCACACGTCTGAACTCCAG,AGAGCACACGTCTGAACTCCAGTCACIIII,ACACGTCTGAACTCCAGTCAC IIIIIAT,GTGCACACGTCTGAACTCCAGTCACIIII,AGCACACGTCTGAACTCCAGTCACIIII,CGTATGCCGTCTTCTGCTTGAAAAA AAAA'`.

Reads were aligned to the human reference genome version hs37d5 with BWA aln⁸⁶ 0.7.12 using parameters `-n 0.01 -o 2 -l 16500`. Mapped reads were further processed with nf-core/eager⁴¹ version 2.5.0, using the config file of the Department of Archaeogenetics in MPI-EVA (https://github.com/MPI-EVA-Archaeogenetics/Autorun_eager/blob/main/conf/Autorun.config). Reads shorter than 30 bp were filtered out, and libraries were deduplicated with picard MarkDuplicates v2.26.0 (<https://broadinstitute.github.io/picard/>). Reads from each sample were merged across libraries. Pseudohaploid genotypes were called with pileupCaller (<https://github.com/stschiff/sequenceTools>) from sequenceTools v1.5.2 using options `-randomHaploid` and `-singleStrandMode`, applying map and base quality filters, and deactivating per-Base-Alignment-Quality (`-Q 30 -q 25 -B`). Genetic sex was determined with Sex.DetERRmine³⁷ on reads filtered with samtools⁶¹ v1.12 for mapping quality 30 and base quality 30.

Imputation

To fill in missing data and obtain diploid genotype calls, samples were imputed. All sequencing data from each individual was collected and used to call diploid genotype likelihoods with ATLAS.⁶² Samples were then imputed using GLIMPSE⁶³ and the 1000 Genomes phase 3 reference panel.⁸⁷ Samples that had posterior genotype probability (GP) ≥ 0.99 on at least 50% of 1240k positions, were included in the downstream IBD analyses. This threshold corresponds roughly to 1X coverage on the captured 1240k positions, or 400,000 SNPs, which is the recommended coverage cutoff for anclBD.²⁴ We note that some samples coverage below 1X while they still yielded sufficient number of SNPs and reasonable imputation results. Thus, we did not want to exclude samples purely based on coverage metrics.

Contamination estimation

We estimated the authenticity of the extracted DNA by measuring the rate of C-to-T substitutions in the 5' ends of the sequencing reads with mapDamage2⁶⁴ v2.2.1. Mitochondrial contamination was estimated using contamMix¹⁴ with the parameter `-trim_bases 2`. Additionally, we estimated mitochondrial contamination with Schmutzi.¹⁵ In one case, PKN007, Schmutzi inferred 45% contamination, but both the endogenous and contaminant sequence were classified in the same haplogroup and the individual's contamMix estimate for contamination was low, and we thus consider it uncontaminated. Autosomal contamination was estimated for genetically male individuals with ANGSD.⁶⁵

Analysis of uniparentally-inherited markers

Mitochondrial haplogroups were called from the output fasta files of Schmutzi. We called consensus sequences for both the inferred endogenous and contaminant sequence, since Schmutzi often flips them, using four different quality thresholds for base calls (20, 30, 40 and 50). We then used Haplogrep 3⁶⁶ to classify all the resulting consensus sequences using human MT DNA Phylogeny (phyлотree-rcrs@17.2). In the cases where the base-quality threshold affected the final classification, we present the result from the most conservative filtering, except for one case (PLN004) where the lower-quality call is supported by a genetic first-degree relative of the individual.

Y-chromosomal haplogroups were called from BAM files with Yleaf,³⁰ which we ran twice to obtain haplogroup classifications relative to both YFull and ISOGG trees (the latter with option `-old`) using read depth parameter `-r 1`.

HapROH, kinship, and ancIBD

We used hapROH²⁵ to infer runs of homozygosity and effective population size. The analysis was done on pseudohaploid data and included only samples with $\geq 400,000$ SNPs. Inferred ROH were used to estimate the population size with a maximum likelihood framework using function *fit_ne* implemented in the hapROH package.

READv2¹⁷ was used to infer close biological relatedness between the ancient individuals from pseudohaploid data for all individual with $>20,000$ SNPs. For robustness, we considered inferred third-degree relations only if the value in the column `Z_upper` (describing how many standard errors the normalized mean P0 score is from a lower degree of relatedness) was above 3.

To examine more distant relatedness between the ancient individuals, we used ancIBD²⁴ to infer IBD sharing between the ancient individuals using imputed data. Imputed genotypes were downsampled to 1240k panel positions, and the fraction of high-probability genotype calls were calculated. Samples that had posterior genotype probability of ≥ 0.99 in $>50\%$ of the sites (`maxGP(0.99) ≥ 0.5`) were included. AncIBD was then run on a large set of published samples to call IBD segments of ≥ 8 cM between all pairs. We constructed an IBD network that included individuals that were either directly connected to at least one of the ancient Pirkanmaa individuals, or indirectly connected to them via one additional individual. We filtered these potential IBD connections using the following conditions: each pair must share at least 2 segments in IBD, and if either individual in a pair had `maxGP(0.99) < 0.8` , we additionally required them to share at least one segment of ≥ 16 cM. The IBD network was then visualised with Cytoscape⁶⁷ using edge-weighted spring embedded layout algorithm with sum of IBD segment lengths per pair as a guiding variable. The final layout was adjusted manually for clearer presentation.

Reference datasets

We merged our newly generated ancient DNA data with published and publicly available ancient and present-day genomes. The genotype data was fetched from the Poseidon community archive and merged with trident forge.⁶⁸

The genetic data from Finland used in this study originates from the National FINRISK Study (FINRISK), which is a population-based study conducted every five years since 1972.⁹ Genetic data from cohorts have been collected since 1992, along with information on the birthplace, parental birthplace, birth year, and native language of the study participants. In this study, we used genetic data from the 1992, 1997, 2002, 2007, and 2012 cohorts and included individuals where both parents were born in the same municipality. We created two reference datasets: The first one, 'THL_WGS', contained the 1240k positions pulled down from samples that had whole-genome sequencing data available. We performed a lift-over from hs38 to hs37 and merged the datasets using PLINK⁶⁹ v1.90b3.29. The final dataset included 281 individuals and 936,564 SNPs. These data were used in F statistics.

To obtain better geographic coverage across Finland, we constructed a second dataset, 'THL_HCE', which was combined from genotyping chip data from the FINRISK cohorts. These included six genotyping batches, all genotyped with Illumina HumanCoreExome genotyping arrays. These data were used only for the IBD analysis.

FINRISK genotyping batches were merged using PLINK. Duplicate positions were removed and strand orientations were checked. Sites where strandedness could not be resolved (i.e. AT/CG sites) were removed. After merging, we obtained a dataset with 466,791 markers and 23,395 individuals. We then removed variants with low genotyping success (`-geno 0.01`), low minor allele frequency (`-maf 0.05`) or Hardy-Weinberg equilibrium *p*-value below 1.0×10^{-6} . We also removed variants in 24 previously reported regions of exceptionally long LD (Price et al. 2008) and individuals with high or low heterozygosity (`|F| ≥ 0.04`) and low genotyping rate (`-mind 0.005`), as well as individuals with over 10% missingness on chromosome 21. We estimated relatedness up to third degree (kinship coefficient threshold 0.0442) in our dataset and pruned related individuals using KING⁷⁰ with default parameters. Finally, we removed genetic outliers by running PCA together with non-Finnish samples from the 1000 Genomes phase 3 pane.⁸⁷ For PCA, we used variants overlapping the 1240k SNP panel ($n = 145,639$). PCA was first conducted on the full dataset and then separately for the

five metapopulations (EUR, EAS, AMR, AFR and SAS). From each of these, we identified outliers by utilizing the k-nearest neighbors ($k = 34$) method as implemented in the Class library in R 4.3.2 (<https://rdocumentation.org/packages/class/versions/7.3-23>). Finnish individuals that were classified into one of the global metapopulations instead of Finnish ($n = 7$) were removed as outliers. The final dataset consisted of 4,722 individuals and 230,708 SNPs.

PCA

We visualised the individuals' ancestry with principal component analysis (PCA) using present-day West Eurasians genotyped with the Human Origins array⁸⁸ (Table S2). We used only pseudohaploid data with projection for ancient individuals. We used the tool smartpca from EIGENSOFT⁷¹ with parameters `lsqproject: YES`, `newshrink: YES` and `popsizelimit: 25`. The populations used for the Eurasian-wide PCA spanning were: Abkhasian, Adygei, Albanian, Armenian, Balkar, Basque, BedouinA, BedouinB, Belarusian, Bulgarian, Canary_Islander, Chechen, Chuvash, Croatian, Cypriot, Czech, Druze, English, Estonian, Finnish, French, Georgian, Greek, Hungarian, Icelandic, Iranian, Italian_North, Italian_South, Jew_Ashkenazi, Jew_Georgian, Jew_Iranian, Jew_Iraqi, Jew_Libyan, Jew_Moroccan, Jew_Tunisian, Jew_Turkish, Jew_Yemenite, Jordanian, Kumyk, Lebanese, Lezgin, Lithuanian, Maltese, Mordovian, Norwegian, Orcadian, Palestinian, Polish, Russia_NorthOssetian.DG, Russian, Sardinian, Saudi, Scottish, Sicilian, Spanish, Spanish_North, Syrian, Turkish, and Ukrainian.

We plotted the results of two different PCAs to visualise the individuals' ancestry within Finland. The first dataset included individuals from the 19 present-day provinces of mainland Finland: Etelä-Karjala, Etelä-Pohjanmaa, Etelä-Savo, Kainuu, Kanta-Häme, Keski-Pohjanmaa, Keski-Suomi, Kymenlaakso, Lappi, Päijät-Häme, Pirkanmaa, Pohjanmaa, Pohjois-Karjala, Pohjois-Pohjanmaa, Pohjois-Savo, Satakunta, Uusimaa, and Varsinais-Suomi. We used the same parameters as above, except the `popsizelimit` was set to 100 to balance the group sizes without losing excess data. Since this PCA mainly separates Finland on its east-west (PC1) and north-south (PC2) axes, we further calculated a second PCA where we only included the 8 southwestern provinces (Kanta-Häme, Keski-Suomi, Kymenlaakso, Päijät-Häme, Pirkanmaa, Satakunta, Uusimaa, Varsinais-Suomi), which were largely overlapping in the first PCA, to obtain better local resolution.

ADMIXTURE

We ran ADMIXTURE¹³ analysis to further visualise the ancestry composition of the ancient individuals relative to modern populations. We used present-day individuals typed with the Human Origins array and pseudohaploid genomes of ancient individuals (Table S2). The input data was pruned using PLINK v1.90b3.29 to exclude markers with minor allele frequency less than 0.01. We then performed LD pruning using `-indep-pairwise` with a window size of 200, a step size of 5 and an R^2 threshold of 0.5. ADMIXTURE was then run for K number of components (K) ranging from 2 to 16. We ran five replicates for each K value and calculated median CV error per K across the replicates. $K=11$ had the lowest CV error. The populations used for the ADMIXTURE analysis were Mbuti, Mbuti.DG, Yoruba, Hadza, Pima, Karitiana, Papuan, Onge, Mixe, Ami.DG, Atayal.DG, Han, Ulchi, Even, Mala, Brahmin_Tiwari, GujaratiB, Makrani, Brahui, Balochi, BedouinB, Kalash, Armenian, Cypriot, Greek, Croatian, Sardinian, Basque, Spanish, French, English, Scottish, Orcadian, Norwegian, Icelandic, Hungarian, Czech, Sorb, Polish, Ukrainian, Ukrainian_North, Belarusian, Lithuanian, Estonian, Finnish, Finnish.DG, Karelian, Veps, Mordovian, Russian_Central, Russian_Archangelsk_Krasnoborsky, Russian_Archangelsk_Leshukonsky, Russian_Archangelsk_Pinezhsky, Chuvash, Udmurt, Mari.SG, Mansi, Mansi.DG, Selkup, Nganasan, Saami.DG, Saami.WGA, TMP002, TMP003, PLN001, PLN002, PLN003, PLN004, PKN002, PKN004, PKN005, PKN006, PKN008, PKN007, PKN010, PKN011, PKN012, PKN013 and PKN014.

F statistics

F statistics were calculated using the `xerxes fstats v1.0.1.1` tool of the Poseidon framework.⁶⁸ Mbuti.DG⁸⁹ was used as an outgroup in all calculations. All F statistics were done on pseudohaploid versions of ancient genomes.

The mean of pairwise F3 estimates within the mediaeval and post-mediaeval group was used to assess differences in genetic diversity over time. Due to the small sample size, we used a permutation test to evaluate whether the mean pairwise-F3 values differed significantly between the two temporal groups. We randomly shuffled group labels of the individuals while maintaining the original group sizes, and calculated the difference in mean F3 values between the two permuted temporal groups. This process was repeated 1,000,000 times to generate a distribution of mean differences under the assumption of no group structure. The statistical significance of the observed difference in means was then assessed by calculating a p-value as the proportion of permuted differences greater than or equal to the observed difference.

IBD connectivity and spatial interpolation

To analyse IBD sharing between ancient and present-day Finns, we used IBIS.⁷² We used the imputed genotypes of the ancient individuals, and filtered them to contain all positions that had $\text{maxGP} \geq 0.99$. Individual data was then merged with the genotypes of the present-day Finns (dataset 'THL_HCE'; Table S4). We analysed each ancient individual separately to avoid cumulative loss of data. The number of SNPs used for the IBD calling was between 115,829 and 195,516. IBIS was run with parameters `-mt 300`, `-er 0.004`, `-maxDist 0.1` and `-min_l 8`. We calculated the sum of segment lengths shared by each pair of ancient and modern individuals, and averaged those sums over municipalities. These values were then used to visualise IBD connectivity over the area of present-day Finland using kriging interpolation as implemented in package `gstat` in R.⁹⁰ We fit a linear model for the variograms using a range

of 200 km for “all” and “common” segment categories, and 150 km for “rare” segments since the spatial pattern of rare segments decays faster. Segments were sorted into these categories based on whether or not they shared exact boundaries (genomic start and end coordinates) with other segments in the combined dataset. Segments that did not share boundaries with other segments (i.e., were only shared by one ancient and one modern individual) were classified as “rare”, whereas all other segments were classified as “common”. We note that this approach is an approximation of the segment’s frequency in the population, since some of the segments classified as “rare” had nearly perfect overlap with other, more frequent segments, but slightly shifted boundaries. This could be due to recombination, but also due to errors in sequencing, imputation or IBD calling.

To visualise IBD connectivity of single individuals, we used inverse distance weighting interpolation (idw from gstat) instead of kriging, as many individuals showed patterns of IBD connectivity that could not be captured by a variogram. We used a coarser prediction grid to average over slightly larger areas, as idw tends to produce “patchy” patterns and emphasise individual data points with high values. The power parameter was set to 1 based on comparison of different parameter values using leave-one-out cross-validation.

Promethease and HirisPlex

Promethease (<https://promethease.com/>) and HirisPlex⁵⁰ are tools commonly used to interpret and predict certain phenotypic traits from genetic data. Promethease provides a personal DNA report by matching user-uploaded raw genetic data to scientific literature, claiming to give insights into health, traits, and ancestry-related information. It cross-references genetic markers with findings from the SNPedia database, allowing users to examine potential genetic predispositions and various traits and conditions.⁹¹

We used imputed genotype data obtain information on variants that may have affected the phenotypic traits of the analysed ancient individuals. We included the 14 individuals that exceeded the threshold for sufficient imputation quality (see [imputation](#) above). We filter sites with posterior genotype probability of 0.99 or higher, and removed other than bi-allelic variants and variants that did not have a stable rSID. Remaining variants were uploaded to Promethease in 23andMe format.

HirisPlex is a predictive tool designed to estimate eye, hair, and skin colour from genetic data. It analyzes specific genetic markers associated with pigmentation, helping to make informed predictions about the phenotype of historical or unidentified individuals. It requires diploid genotype calls, which were obtained from the raw allele counts on the Hirisplex positions by manual inspection.

Pathogen screening

To assess the health of the individuals, we screened the samples for potential human pathogen DNA, which could be indicative of infections of the individuals analysed in this study. All the sequencing reads were processed with AdapterRemoval⁹² v.2.3.1 to trim adapters with a minimum overlap of 1 base (–minoverlap 1), merge pair-end reads and filter any reads shorter than 30 base pairs (–minlength 30) and/or a quality lower than 20 (–minquality 20). The adapter-trimmed and filtered reads were run through two automatic pipelines: a general screening pipeline for human pathogens that included 671 taxonomic ranks that can cause disease in humans ([Table S12](#)) and a specific *Yersinia pestis*, the aetiological agent of plague, screening pipeline based on the method presented in [Andrades Valtueña et al.](#)⁴²

In the general screening pipeline, the reads were mapped against a multifasta reference containing a representative for the pathogens (the species rank in [Table S12](#)) with bwa aln (v0.7.12) with default parameters except for -n 0.01 -l 16. The mapped reads were then extracted from the bam file with samtools v1.3 view command and subsequently transformed to fastq file with samtools fastq. The resulting fastq files were run through the Autorun_deepscreening pipeline (https://github.com/MPI-EVA-Archaeogenetics/Autorun_deepscreening). In short, fastq files were processed with nf-core/eager⁴¹ v.2.4.7 with the following command:

```
nextflow run nf-core/eager -r 2.4.7 -c Autorun_deepscreening.config -p eva,archgen,autorun,local_paths,Bacterial_Viral_Prescreening -input input.tsv -output .
```

The config file can be found in https://github.com/MPI-EVA-Archaeogenetics/Autorun_deepscreening/blob/main/conf/Autorun_deepscreening.config. Within nf-core/eager the reads were aligned to the PhiX genome (NC_001422.1) and the non-mapping reads were then aligned and taxonomically classified with MALT^{73,93} to a database containing a single representative for all the bacterial genomes found in the NCBI dataset as of January 2023. HOPS⁴⁰ as implemented in nf-core/eager was then used to detect and authenticate pathogen candidates. HOPS uses three criteria for authentication and assigns a rank to potential matches: 1 - decreasing edit distance compared to the reference, 2 - presence of substitutions in congruence with DNA damage (C>T substitution in 5’ and G>A substitutions in 3’) and 3 - decreasing edit distance in reads displaying substitutions typical of aDNA. We consider only rank 3 matches reliable and discuss them in the results. All matches regardless of rank are presented in [Table S13](#).

Additionally, the trimmed and filtered fastq were run through an automatic pipeline to detect the presence of *Yersinia pestis*, based on the competitive mapping screening strategy presented in [Andrades Valtueña et al.](#)⁴² In short, reads are aligned with bwa aln with the parameters described above to a multifasta reference containing the genomes of 13 *Yersinia* species, including *Yersinia pestis* CO92 and its three plasmids pCD1, pMT1 and pPCP1. The latter two are exclusive to *Y. pestis*. Reads mapping to more than one location (mapping quality of 0) are discarded with samtools view, and samtools faidx is used to calculate the number of mapping reads for each entry in the multifasta file. A score is calculated based on the number of uniquely mapping reads to *Y. pestis* (YPS) and the maximum reads mapping to any other *Yersinia* (YS) normalised by the number of input reads for mapping (M) as follows:

$$(YPS - \max(YS))M \times 1000.$$

Samples with a score above 0.001 are considered potential candidates for *Yersinia pestis*. Additionally, samples with presence in all of the *Y. pestis* plasmids, regardless of their score, are considered potential candidates for this bacterium.